

**UNCLASSIFIED**

---

---

**AD. 278 717**

*Reproduced  
by the*

**ARMED SERVICES TECHNICAL INFORMATION AGENCY  
ARLINGTON HALL STATION  
ARLINGTON 12, VIRGINIA**



---

---

**UNCLASSIFIED**

NOTICE: When government or other drawings, specifications or other data are used for any purpose other than in connection with a definitely related government procurement operation, the U. S. Government thereby incurs no responsibility, nor any obligation whatsoever; and the fact that the Government may have formulated, furnished, or in any way supplied the said drawings, specifications, or other data is not to be regarded by implication or otherwise as in any manner licensing the holder or any other person or corporation, or conveying any rights or permission to manufacture, use or sell any patented invention that may in any way be related thereto.

RADC-TDR-62-130

### Technical Note 3

# THE DESIGN OF BRANCH GUIDE DIRECTIONAL COUPLERS FOR LOW AND HIGH POWER APPLICATIONS

Prepared for:

ROME AIR DEVELOPMENT CENTER  
AIR FORCE SYSTEMS COMMAND  
UNITED STATES AIR FORCE  
GRIFFISS AIR FORCE BASE, NEW YORK

CONTRACT AF 30(602)-2392

By: Leo Young

STANFORD RESEARCH INSTITUTE

MENLO PARK, CALIFORNIA

\*SRI

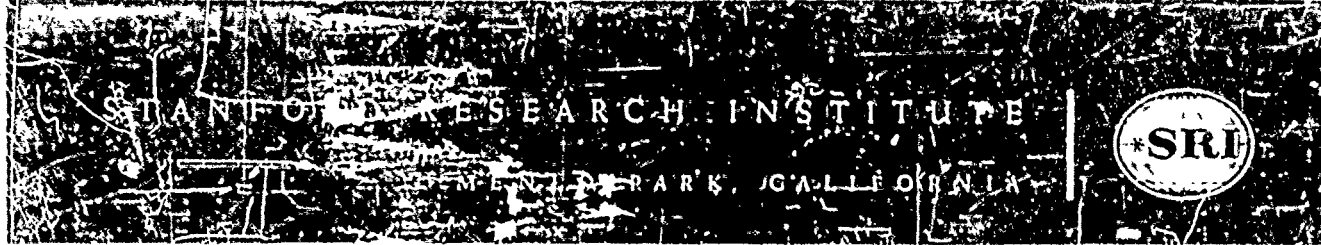
278717

## NOTICES

When Government drawings, specifications, or other data are used for any purpose other than in connection with a definitely related Government procurement operation, the United States Government thereby incurs no responsibility nor any obligation whatsoever; and the fact that the Government may have formulated, furnished, or in any way supplied the said drawings, specifications, or any other data, is not to be regarded by implication or otherwise as in any manner licensing the holder or any other person or corporation, or conveying any rights or permission to manufacture, use, or sell any patented invention that may in any way be related thereto.

Qualified requestors may obtain copies of this report from the ASTIA Document Service Center, Arlington Hall Station, Arlington 12, Virginia. ASTIA Services for the Department of Defense contractors are available through the "Field of Interest Register" on a "need-to-know" certified by the cognizant military agency of their project or contract.

This report has been released to the Office of Technical Services, U.S. Department of Commerce, Washington 25, D.C., for sale to the general public.



February 1962

RADC-TDR-62-130

Technical Note 3

## THE DESIGN OF BRANCH GUIDE DIRECTIONAL COUPLERS FOR LOW AND HIGH POWER APPLICATIONS

Prepared for:

ROME AIR DEVELOPMENT CENTER  
AIR FORCE SYSTEMS COMMAND  
UNITED STATES AIR FORCE  
GRIFFISS AIR FORCE BASE, NEW YORK

CONTRACT AF 30(602)-2392

By: Leo Young

SRI Project No. 3478

Approved:

*G. L. Matthei*  
G. L. MATTHEI NPD MICROWAVE GROUP

*D. R. Scheuch*  
D. R. SCHEUCH, DIRECTOR ELECTRONICS AND RADIO SCIENCES DIVISION

Copy No. 23

## FOREWORD

---

This is Technical Note 3 issued on Contract AF 30(602)-2392, conducted by the Electromagnetics Laboratory of Stanford Research Institute and sponsored by the Rome Air Development Center. The program started on 29 November 1960. Mr. Robert Powers serves as the technical monitor on this contract.

The author wishes to acknowledge the contributions of M. D. Domenico, who carried out the measurements; P. H. Omlo and Suzanne B. Philp, who compiled the computer program; and D. A. Barrett who helped with the chart calculations.

## ABSTRACT

---

Branch-guide directional couplers can be built in most types of transmission line. A design procedure is here developed which gives predictable and superior performance over a specified frequency band. A new chart was constructed from which the coupler impedances or admittances can be calculated quickly and with sufficient accuracy for nearly all practical applications. Numerical tables are also presented from which most practical cases can be worked out by interpolation.

A five-branch, 6-db coupler and a thirteen-branch, 0-db coupler were constructed in waveguide. The measured points and computed curves were in excellent agreement. Over the frequency band of 1300  $\pm$  130 megacycles, the 0-db coupler had a VSWR of less than 1.07, its insertion loss was better than 0.05 db, and the couplings into the two remaining arms were weaker than 20 db. This coupler can pass at least 5 megawatts of peak power in air at atmospheric pressure.

A 0-db coupler can be used to separate the fundamental frequency power generated by a high-power transmitter from its harmonic frequencies, which couple only weakly through the branches. Most of the harmonic power goes into the load placed in line with the input. Chokes were cut into the branch arms to reduce the cross-coupling in the second harmonic frequency band.

## CONTENTS

---

I	INTRODUCTION . . . . .	1
II	THE QUARTER-WAVE TRANSFORMER PROTOTYPE CIRCUIT . . . . .	4
III	DESIGN BY CHARTS . . . . .	8
IV	CHOICE OF QUARTER-WAVE TRANSFORMER PROTOTYPE . . . . .	18
V	FURTHER NUMERICAL EXAMPLES . . . . .	28
VI	PERIODIC AND SYNCHRONOUS COUPLERS . . . . .	38
VII	EXPERIMENTAL RESULTS . . . . .	46
A.	The 6-db Coupler . . . . .	46
1.	Construction . . . . .	46
2.	Power-Handling Capacity . . . . .	51
B.	The 0-db Coupler . . . . .	51
1.	Construction . . . . .	51
2.	Power-Handling Capacity . . . . .	52
3.	Absorption of Higher Frequencies . . . . .	54
VIII	CONCLUSION . . . . .	62

## ILLUSTRATIONS

---

Fig. 1 Branch-Guide Coupler Cross-Sections—(a), $n = \text{odd}$ , (b), $n = \text{even}$ . . . . .	2
Fig. 2 Branch-Guide Coupler Notation . . . . .	4
Fig. 3 Equivalent Circuit of $i$ th T-Junction for Even or Odd Mode at Center Frequency . . . . .	5
Fig. 4 Spacings Between Branches for Synchronous Couplers . . . . .	6
Fig. 5 Design Chart for Branch-Guide Coupler—Complete Chart . . . . .	9
Fig. 6 Design Chart for Branch-Guide Coupler—Center Expanded to VSWR = 2.0 . . . . .	10
Fig. 7 Design Chart for Branch-Guide Coupler—Center Expanded to VSWR = 1.25 . . . . .	11
Fig. 8 Even- or Odd-Mode Equivalent Circuit for Design of Four-Branch ( $n = 3$ ) Coupler Used in Example III-1 . . . . .	12
Fig. 9 Solution by Chart of Four-Branch ( $n = 3$ ) Coupler Used in Example III-1 . . . . .	13
Fig. 10 Even- or Odd-Mode Equivalent Circuit for Design of Five-Branch ( $n = 4$ ) Coupler Used in Example III-2 . . . . .	16
Fig. 11 Solution by Chart of Five-Branch ( $n = 4$ ) Coupler Used in Example III-2 . . . . .	17
Fig. 12 Plot of Center Frequency Coupling $G$ (db) vs. Impedance Ratio Parameter, $R$ , for a Matched Coupler . . . . .	20
Fig. 13 Best Estimates for Bandwidth Contraction Factor, $\beta_1$ , Based on 27 Individual Solutions . . . . .	22
Fig. 14 VSWR Characteristics of Some Maximally Flat Couplers . . . . .	24
Fig. 15 Directivity Characteristics of Some Maximally Flat Couplers . . . . .	25
Fig. 16 Coupling Characteristics of Some Maximally Flat Couplers . . . . .	26
Fig. 17 Computed Performance of Three-Branch ( $n = 2$ ) Coupler of Example IV-1 . . . . .	27
Fig. 18 Performance of Five-Branch ( $n = 4$ ) Coupler of Example V-1 . . . . .	30
Fig. 19 Insertion Loss $P_2$ (db) and VSWR of 0-db Coupler of Example V-2 . . . . .	32
Fig. 20 Directivity $D$ and In-Line Coupling $P_1$ of 0-db Coupler of Example V-2 . . . . .	33
Fig. 21 Computed Performance of 0-db Coupler with Branches $3\lambda/4$ Long (Example V-3) . . . . .	34
Fig. 22 Computed Performance of Three-Branch ( $n = 2$ ) Coupler of Example V-4 . . . . .	37
Fig. 23 VSWR Characteristics of Four 0-db Couplers . . . . .	39
Fig. 24 Insertion Loss Characteristics of Four 0-db Couplers . . . . .	40
Fig. 25 Computed Performance of Two Eight-Branch 0-db Periodic Couplers . . . . .	45

## ILLUSTRATIONS

Fig.	26 Equivalent Circuits of T-junctions (a) Symmetrical Junction, After Marcuvitz, <sup>17</sup> (b) Unsymmetrical Junction . . . . .	46
Fig.	27 Dimensions of First S-Band 6-db Coupler—Based on Example V-1 . . . . .	48
Fig.	28 Exploded View of 6-db Experimental Coupler . . . . .	49
Fig.	29 Dimensions of S-Band 6-db Coupler After Modifications . . . . .	50
Fig.	30 Dimensions of 0-db Coupler . . . . .	52
Fig.	31 Exploded View of First 0-db Experimental Coupler . . . . .	53
Fig.	32 Arrangement of 0-db Coupler and Spurious-Frequency Rejection Filter . . . . .	54
Fig.	33 Dimensions of 0-db Coupler with Second-Harmonic Chokes . . . . .	55
Fig.	34 Exploded View of 0-db Coupler with Second-Harmonic Chokes . . . . .	56
Fig.	35 Measured Insertion Loss of 0-db Coupler with Second-Harmonic Chokes . . . . .	57
Fig.	36 Arrangement of Ten 3-db Couplers to Suppress Spurious Frequencies . . . . .	57
Fig.	37 View of Complete Filter for Suppression of Spurious Frequencies, Showing Branch-Guide Couplers (Middle), Waveguide Tapers (Foreground and Upper Right), and Waffle-Iron Filter (Upper Left) . . . . .	59
Fig.	38 Incident and Reflected Power in the $T\Theta_{10}$ Mode from the Second to the Eleventh Harmonic with the Filter of Fig. 37 . . . . .	60
Fig.	II-1 Several Matched-Directional Couplers in Cascade . . . . .	73
Fig.	II-2 Summary of Even- and Odd-Mode Analysis . . . . .	73
Fig.	III-1 Transmixing-line Stub in the Mid-Plane of a Line One-Quarter-Wavelength Long . . . . .	74
Fig.	III-2 Smith Chart Procedure to Find $Z_3$ of Fig. III-1 to Match the Stub $Z_2$ . . . . .	76

## TABLES

---

Table I Table Connecting the Impedance Ratio Parameter $R$ with the Coupling $G$ (db) at Center Frequency for a Matched Coupler . . . . .	21
Table II Impedances of Three Synchronously Derived 0-db Couplers . . . . .	42
Table III Maximum VSWR of Several 0-db Couplers Over Stated Bandwidths . . . . .	42
Table IV Maximum Insertion Loss (db) of Several 0-db Couplers Over Stated Bandwidths . . . . .	42
Table V Impedances of Three Synchronous 3-db Couplers . . . . .	43
Table VI Maximum VSWR of Several 3-db Couplers Over Stated Bandwidths . . . . .	43
Table VII Coupling Unbalance (db) of Several 3-db Couplers Over Stated Bandwidths . . . . .	44
Table I-1 Branch-Guide Coupler Impedances for $n = 1$ Section (Two Branches) . . . . .	45
Table I-2 Impedances of Maximally Flat Branch-Guide Couplers from $n = 2$ to 8 Sections (Three to Nine Branches) . . . . .	49
Table I-3 Impedances of Branch-Guide Couplers for $n = 2, 3$ and 4 Sections (Three, Four, and Five Branches) when $v_g = 0.20$ . . . . .	56
Table I-4 Impedances of Branch-Guide Couplers for $n = 2, 3$ and 4 Sections (Three, Four, and Five Branches) when $v_g = 0.40$ . . . . .	57
Table I-5 Impedances of Branch-Guide Couplers for $n = 2, 3$ and 4 Sections (Three, Four, and Five Branches) when $v_g = 0.60$ . . . . .	58
Table I-6 Impedances of Branch-Guide Couplers for $n = 2, 3$ and 4 Sections (Three, Four, and Five Branches) when $v_g = 0.80$ . . . . .	59
Table I-7 Impedances of Branch-Guide Couplers for $n = 2, 3$ and 4 Sections (Three, Four, and Five Branches) when $v_g = 1.00$ . . . . .	60
Table I-8 Impedances of Branch-Guide Couplers for $n = 2, 3$ and 4 Sections (Three, Four, and Five Branches) when $v_g = 1.20$ . . . . .	61

## APPENDICES

---

I Tables of Branch-Guide Coupler Impedances . . . . .	64
II Coupling Formulas for Cascaded Matched Directional Couplers . . . . .	72
III Calculation of Chokes in Branches . . . . .	74

## I INTRODUCTION

The principal objective of this work was to develop a high-power, 0-db, directional coupler in waveguide. This directional coupler was further required to have a configuration that would allow most spurious frequencies to pass into one or another of the two dummy loads.

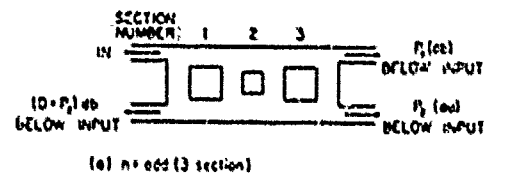
Directional couplers at UHF and microwave frequencies take many forms and have many applications. The branch-guide directional coupler, which is the one investigated here, is suitable for construction in almost any kind of transmission line. In waveguide, its mechanical configuration and its electrical performance are similar to those of Riblet short-slot couplers, or of multihole couplers; in coaxial line or strip-line (where only TEM modes exist), the coupler does not have any such close counterparts. Branch-guide couplers have the following useful combination of properties:

- (1) The coupling between the two lines is through joining branch-lines of finite length, and not through apertures. This gives additional flexibility in design; e.g., special-purpose chokes or filters can be placed in the branches.
- (2) A branch-guide coupler can be designed either as a periodic structure, or as a band-pass filter; as a band-pass filter, its electrical behavior can be optimized over the pass band.
- (3) The number of branches can be increased systematically to improve the electrical performance.
- (4) The coupler is better suited for strong coupling (stronger than 20 db) than weak coupling; 0-db couplers are feasible over large bandwidths.
- (5) In waveguide, the coupler *E*-plane cross-section is constant. It can therefore be milled in two blocks and assembled by the "split-block" construction. Other components can also be milled into the same block.
- (6) The coupler fits into a rectangle; the four output lines are parallel (Fig. 1).
- (7) Branch-guide couplers are capable of handling high RF powers.

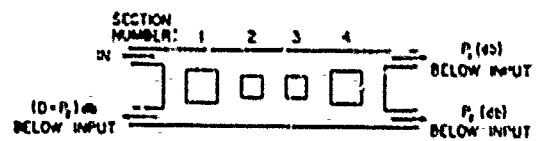
(8) They compare favorably with most couplers as regards VSWR, directivity, and constant coupling over large bandwidths.

In this report a design procedure is worked out, based on the quarter-wave transformer as a prototype circuit, which comes close to being a true synthesis procedure: it enables the designer to work out the physical dimensions of his coupler to meet his performance specification with little or no subsequent need for experimental adjustment.

A short review of the literature on branch-guide couplers will indicate the state of the art. The idea of the even and odd mode analysis of couplers having this kind of symmetry (between upper and lower halves in Fig. 1) goes back at least as far as a war-time report by Lippman.<sup>1</sup> This method of analysis has also been explained in several more recent publications,<sup>2,3</sup> and is indicated in Appendix II (Fig. II-1). The superposition of the even and odd modes, each of which can be solved separately as a loaded-transmission-line (or two-port) problem, then represents the actual directional coupler (or four-port) situation with the generator connected to only a single input. The paper by Reed and Wheeler<sup>2</sup> compares the performance of branch-guide couplers with that of hybrid rings. A later paper by Reed<sup>4</sup> gives general formulas and the results of many calculations on numerous branch-guide couplers, particularly with 0-db coupling. These two papers consider only periodic couplers with uniform main-line, that is to say, the branch impedances are all the same except possibly for the end branches, and the main-line impedance is constant from input to output. Such couplers have some of the advantages and disadvantages of periodic structures: they are simpler to construct than



(a)  $n = \text{odd}$  (3 section)



(b)  $n = \text{even}$  (4 section)

FIG. 1 BRANCH-GUIDE COUPLER CROSS-SECTIONS.  
(a)  $n = \text{odd}$ , (b)  $n = \text{even}$

<sup>1</sup> References are listed at the end of the report.

less regular structures, but they have no clearly defined pass band in which the optimum performance is sought or realized. To realize such band-pass behavior, a filter rather than a periodic structure is needed, and the branch and main line impedances have to be controlled separately. Lomar and Crompton<sup>3</sup> have described an experimental five-branch "binomial" coupler, in which only the branch impedances were adjusted, the main line still being of uniform impedance. Their approach is based on a first-order theory,<sup>4</sup> in which any coupler is considered as a cascaded set of two-branch couplers; extensive empirical changes have to be made experimentally to obtain the desired performance. Young<sup>5</sup> has considered the general case when the branch- and main-line impedances are both allowed to vary. He has given formulas ensuring perfect match and perfect directivity as well as the correct coupling at a single frequency.

This report supplies an optimization procedure over a given pass band. The performance of many designs was analyzed on a digital computer to check out the theory. Compared to periodic couplers,<sup>2,4</sup> only about half as many branches are generally required to give about the same pass-band performance. One 6-db and one 0-db coupler were built in waveguide, with very close agreement between experimental results and predicted performance.

## II THE QUARTER-WAVE TRANSFORMER PROTOTYPE CIRCUIT

A prototype circuit may be defined as a circuit that can be designed to have certain desired electrical characteristics, and that can in some manner be transformed into another circuit having the desired mechanical characteristics while retaining at least approximately the desired electrical characteristics. The prototype circuit is usually in such a form that it can readily be synthesized to meet the electrical performance specifications.

A well-known prototype situation is the transformation of lumped-constant low-pass filters<sup>1,2</sup> into band-pass filters, both lumped-constant and microwave. Another example is the quarter-wave transformer,<sup>3</sup> which can be transformed into half-wave filters and direct-coupled-cavity filters. The general synthesis procedure for quarter-wave transformers is known<sup>10,11</sup> and numerical tables of solutions have been published.<sup>12</sup> An extensive review with many more tables has been presented in a recent SHI report.<sup>13</sup> The quarter-wave transformer can also be used as a prototype circuit for branch-guide couplers, by appropriately relating the steps of the transformer to the T-junctions of the coupler. The notation for the branch-guide coupler impedances or admittances is shown in Fig. 2. For shunt stubs an admittance representation is used, and for series stubs an impedance representation. Each T-junction becomes a one-eighth-wavelength (or 45 degree) stub in both the even and the odd-mode, open-circuited in the one case and short-circuited in the other, as shown in Fig. 3. Only the shunt case is shown in the lower half of

$K_0$	$K_1$	$K_2$	---	$K_{i-1}$	$K_i$	$K_{i+1}$	---	$K_n = K_1$	$K_{n+1} = K_0$
$H_1$	$H_2$	---		$H_{i-1}$	$H_i$	$H_{i+1}$	---	$H_{n+1} = H_1$	
$K_0$	$K_1$	$K_2$	---	$K_{i-1}$	$K_i$	$K_{i+1}$	---	$K_n = K_1$	$K_{n+1} = K_0$

FIG. 2 BRANCH-GUIDE COUPLER NOTATION

Fig. 3. Then the 45 degree stub becomes a shunt admittance  $\pm jH_i$  at the  $i$ th junction counting from either side. The line admittances on either side are  $K_{i-1}$  and  $K_i$ , respectively. The dual of the coupler with shunt junctions is the coupler with series junctions, in which all  $H$  and  $K$  are impedances. Since we wish to include both cases in one discussion, we shall (following Bode<sup>14</sup>) refer to  $H$  and  $K$  as admittances, meaning admittances when there are shunt junctions, and impedances when there are series junctions. The two nearest reference planes with real reflection coefficient  $\Gamma_i$  are shown in Fig. 3 at distances  $\phi'_i$  to the left and  $\phi''_i$  to the right of the junction. Without loss in generality, we may suppose

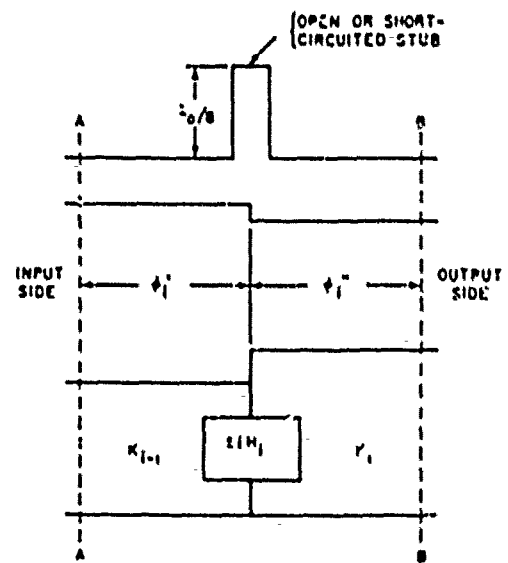


FIG. 3 EQUIVALENT CIRCUIT OF AN T-JUNCTION FOR EVEN OR ODD MODE AT CENTER FREQUENCY

$$K_i > K_{i-1} \quad \dots \quad (1)$$

Then it can be shown (for instance, by referring to a Smith chart) that

$$0 \leq \phi'_i \leq \phi''_i \leq 90^\circ, \quad \text{when } H_i > 0 \quad (2a)$$

and

$$0 \leq \phi''_i \leq \phi'_i \leq 90^\circ, \quad \text{when } H_i < 0 \quad (2b)$$

The values of  $\phi'_i$  and  $\phi''_i$  are given in terms of  $H_i$ ,  $K_{i-1}$  and  $K_i$  by

$$\phi'_i = \frac{1}{2} \arctan \left\{ \frac{2H_i K_{i-1}}{H_i^2 + K_i^2 - K_{i-1}^2} \right\} \quad (3)$$

$$\phi''_i = \frac{1}{2} \arctan \left\{ \frac{2H_i K_i}{H_i^2 + K_{i-1}^2 - K_i^2} \right\}$$

Furthermore, when  $H_i$  is positive, and when the right-hand (high- $K$ ) side is matched, then the normalized admittance looking into the reference plane  $A$  on the left-hand (low- $K$ ) side is real and greater than unity; when the left-hand (low- $K$ ) side is matched, then the normalized admittance looking into the reference plane  $B$  on the right-hand (high- $K$ ) side is likewise real and greater than unity. However, when  $H_i$  is negative the normalized admittances seen in the two nearest reference planes  $A$  and  $B$  are real but less than unity. (These results can all be proved by consulting a Smith chart.)

The junction VSWR<sup>11,12</sup>,  $V_i$ , is given by

$$V_i = \frac{[(K_i + K_{i-1})^2 + H_i^2]^{\frac{1}{2}} + [(K_i - K_{i-1})^2 + H_i^2]^{\frac{1}{2}}}{[(K_i + K_{i-1})^2 + H_i^2]^{\frac{1}{2}} - [(K_i - K_{i-1})^2 + H_i^2]^{\frac{1}{2}}}. \quad (4)$$

A sequence of junctions like the one shown in Fig. 3 (shunt case) is shown in Fig. 4. It represents a portion of one-half the branch-guide coupler in either the even or odd mode (either all  $H_i$  positive or all  $H_i$  negative). If the branch-guide coupler (i.e., the circuit of Fig. 4) is to be based on the quarter-wave transformer, reference planes on opposite sides of adjacent junctions must touch<sup>13</sup> as shown in Fig. 4, which is the

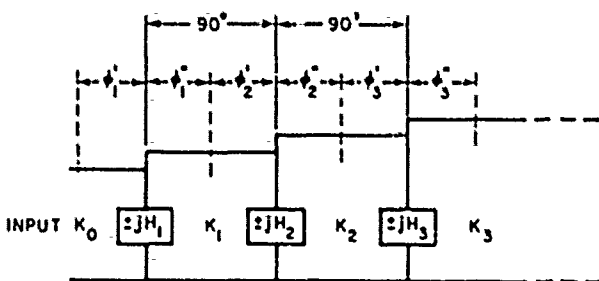


FIG. 4 SPACINGS BETWEEN BRANCHES FOR SYNCHRONOUS COUPLERS

<sup>13</sup>This is possible for both the even and the odd modes simultaneously when the branch lengths and the branch spacings are all one-quarter wavelength. It is probably not possible in any other case.

synchronous-tuning condition<sup>13</sup> for filters. Branch-guide couplers designed in this manner will therefore be called synchronous couplers.

In addition, the junction VSWRs,  $V_j$ , of the coupler must be set equal to the  $V_j$  of the selected prototype transformer, which gives a condition connecting  $K_j$ ,  $K_{j-1}$  and  $H_j$ . (Only their ratios, and not the impedance level, are significant, so that only two and not three quantities have to be solved for.) The other condition derives from the reference-plane positions. Since the coupler is symmetrical about the center, the position of the reference plane associated with the center branch or pair of branches depends on whether the number of sections,  $n$ , is odd or even (Fig. 1). (The number of branches is one more than the number of sections, that is,  $n + 1$ .)

For  $n = \text{odd}$  (Fig. 1a)—Suppose that for instance  $n = 3$ . There are thus four branches. The center reference plane at band center is by symmetry 45 degrees from its junction, which in this case is the second junction from the end. Once a three-section quarter-wave transformer prototype has been selected,  $V_j$  of this prototype transformer can be calculated. For  $n = 3$ , or any odd  $n$ ,  $\phi_j'' = 45^\circ$ , and from Eqs. (3) and (4) the parameters of this junction,  $K_1/K_2$ ,  $H_2/K_2$  and  $\phi_1'$ , can now be deduced. This in turn yields  $\phi_1'' = 90^\circ - \phi_2'$ , which, when  $V_j$  of the prototype transformer is known, yields the required parameters of the first junction,  $K_0/K_1$  and  $H_1/K_1$ , from Eqs. (3) and (4).

For  $n = \text{even}$  (Fig. 1b)—Suppose that for instance  $n = 4$ . There are thus five branches. The center branch, of immittance  $H_3$ , has the same immittance  $K_2$  on either side of it, since  $n$  is even. The VSWR of the immittance  $(1 + jH_3/K_2)$  is set equal to the junction VSWR,  $V_j$ , of the middle step (the third step from either end) of the appropriate four-section quarter-wave transformer prototype circuit. This determines  $H_3/K_2$  and also  $\phi_3' = \phi_3''$  of the middle junction. From the next junction VSWR,  $V_j$ , of the prototype transformer and the equation  $\phi_3'' = 90^\circ - \phi_2'$ , the parameters of the second T-junction are obtained from Eqs. (3) and (4), yielding  $K_1/K_2$ ,  $H_2/K_2$  and  $\phi_1'$ , and so on down the line.

Since this procedure is numerically tedious, a graphical solution was devised, which depends on a sort of Smith chart<sup>15</sup> crossed with a Carter chart.<sup>16</sup> The graphical solution is described in the next section.

### III DESIGN BY CHARTS

The three charts shown in Figs. 5, 6, and 7 are, respectively, the full chart and two charts with an expanded center. (Figure 7 is more expanded than Fig. 6.) The lower circle in Fig. 5 contains the portion of a Smith chart inside the unit conductance (or resistance) circle. There are two families of circles outside. One is the family of constant conductance<sup>\*</sup> circles, with the reciprocal values marked; thus inside the Smith-chart circle the conductances have been selected to have values 1.2, 1.4, 1.6, etc., while those outside are marked likewise but have conductance 1/1.2, 1/1.4, 1/1.6, etc. (instead of the usual circles of conductances 0.8, 0.6, etc.). The other family of circles represents contours of  $\arg Y = \text{constant}$  where  $Y$  stands for admittance. If we write  $Y = G + jB$ , then the number of degrees represent the quantity  $\text{arc tan}(B/G)$ . The use of this chart will now be explained by means of two examples, and the theory behind it will become apparent as the explanation proceeds.

*Example III-1—Case of  $n = \text{odd}$ .* Design a branch-guide coupler based on a quarter-wave transformer of  $n = 3$  sections, output-to-input impedance ratio  $R = 6$ , and transformer fractional bandwidth<sup>†</sup>  $\nu_g = 0.6$  (The selection of the prototype is dealt with later.)

From the tables,<sup>12</sup> the junction VSWRs of the prototype transformer are  $V_1 = 1.311$  and  $V_2 = 2.4495/1.311 = 1.869$ . Half the coupler for either the even or the odd mode is shown in Fig. 8.

<sup>\*</sup> To simplify the explanation, only conductance and susceptance will be used (corresponding to shunt branches); the statements are however equally true on the dual impedance basis (corresponding to series branches).

<sup>†</sup> The transformer fractional bandwidth is defined as usual by

$$\nu_g = \frac{\lambda'_{g1} - \lambda'_{g2}}{\lambda'_{g1} + \lambda'_{g2}}$$

where  $\lambda'_{g1}$  and  $\lambda'_{g2}$  are the longest and shortest guide wavelengths in the quarter-wave-transformer pass band.<sup>12</sup> Its center-frequency is determined from the guide wavelength  $\lambda'_{g0}$  at center frequency, given by

$$\lambda'_{g0} = \frac{2\lambda'_{g1}\lambda'_{g2}}{\lambda'_{g1} + \lambda'_{g2}}.$$

The response is symmetrical about this point when plotted against  $\lambda'_{g0}/\lambda'_g$ .

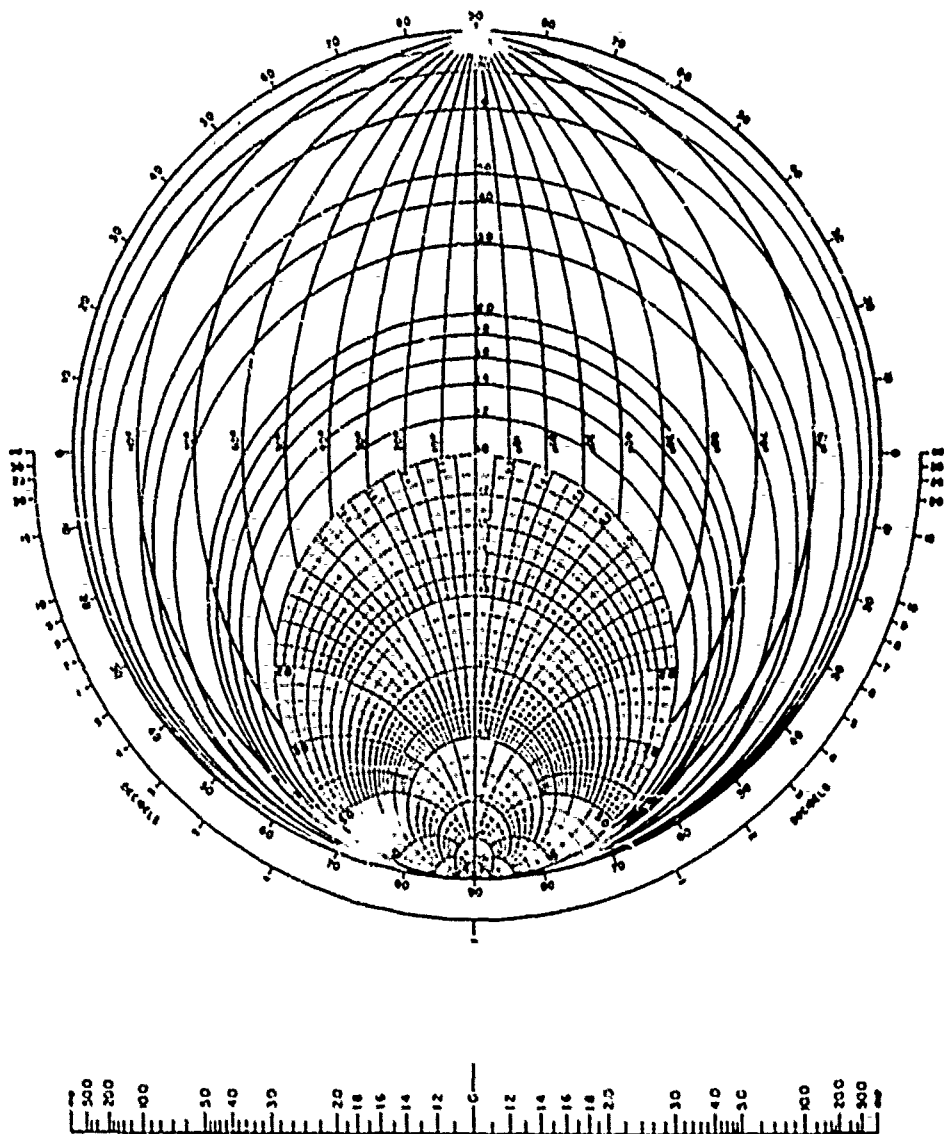


FIG. 5 DESIGN CHART FOR BRANCH-GUIDE COUPLER - COMPLETE CHART

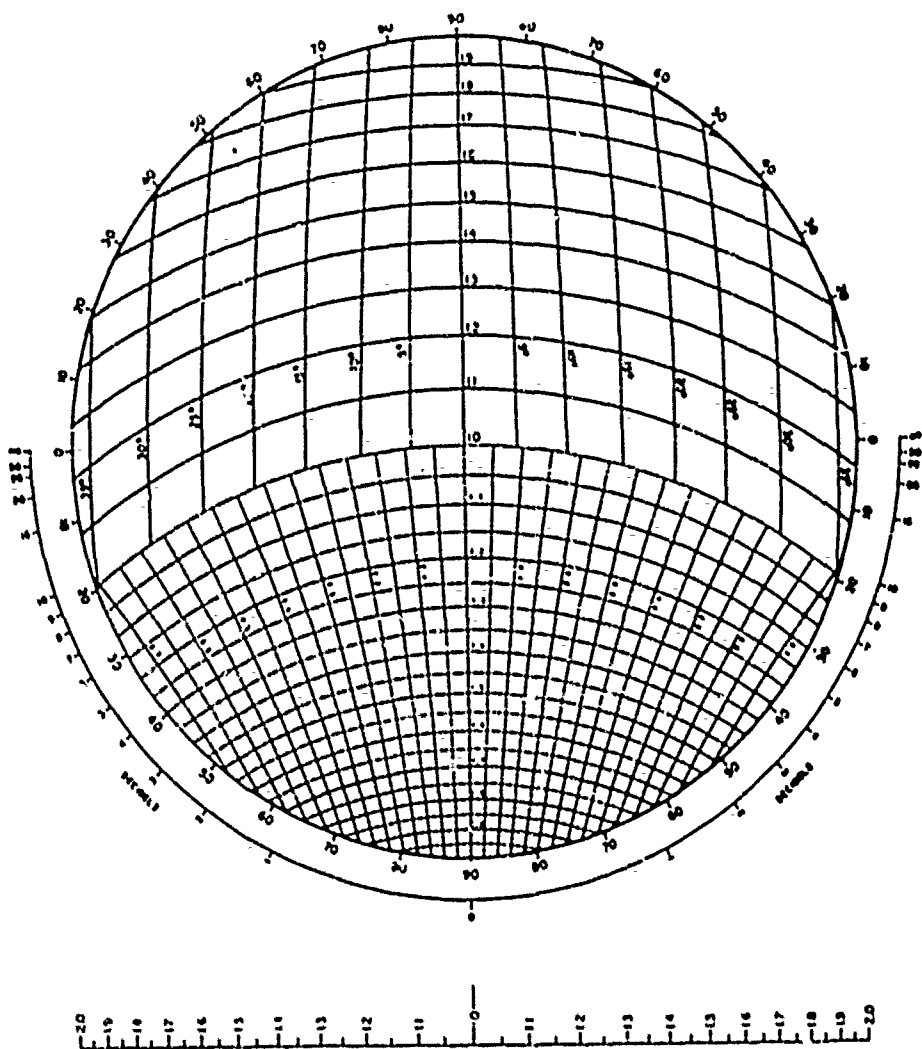


FIG. 6 DESIGN CHART FOR BRANCH-GUIDE COUPLER - CENTER EXPANDED  
TO VSWR = 2.0

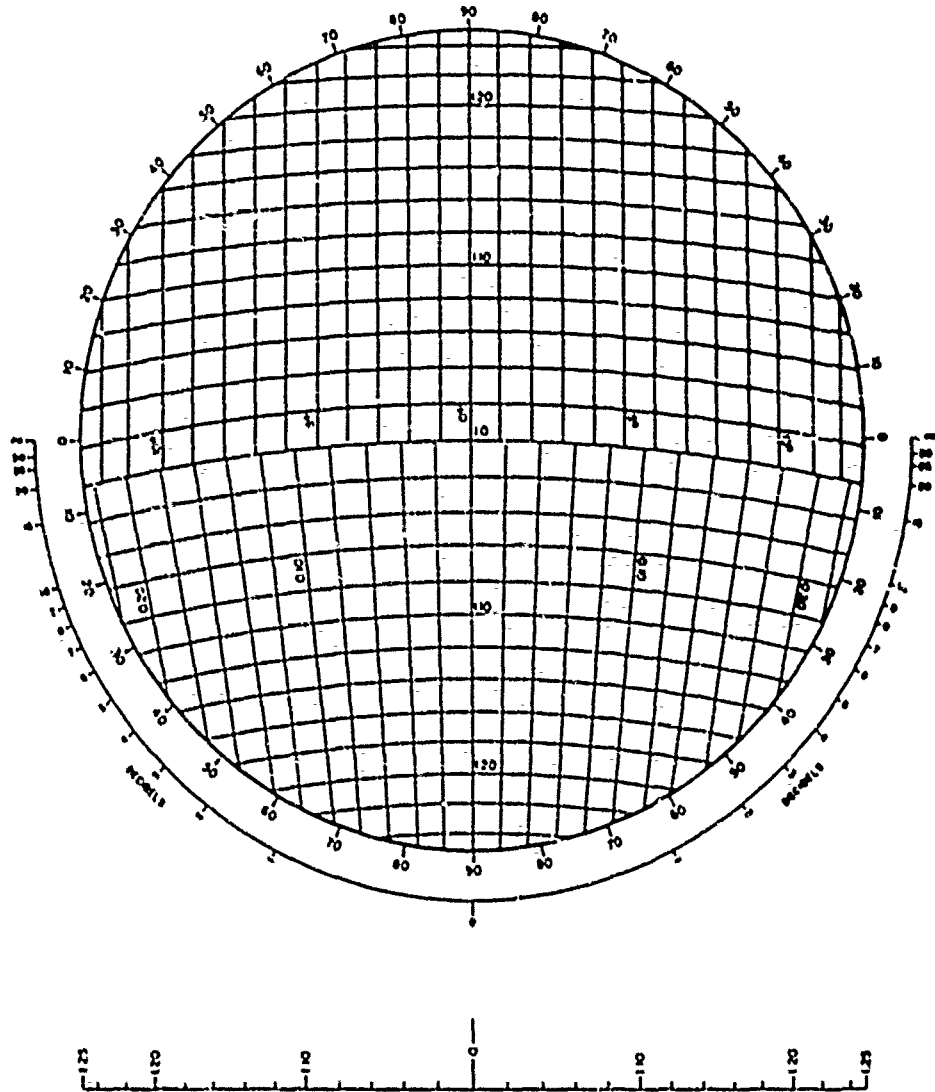


FIG. 7 DESIGN CHART FOR BRANCH-GUIDE COUPLER - CENTER EXPANDED TO VSWR = 1.25

The second junction from the end is 45 degrees from the reference plane at the center of the coupler, where the reflection coefficient of this junction ( $\Gamma_2$ ) is real. Therefore in the plane of the junction,  $\Gamma_2$  is pure imaginary (since it is 45 degrees from  $\Gamma_1$  = real), and this  $\Gamma_2$  is therefore on the horizontal diameter in Fig. 9. Its position is determined by  $V_2 = 1.869$ , and it is located at the point marked "START." It corresponds to the normalized admittance  $(K_1 + jH_2)/K_2$ .

Next we wish to find the admittance  $A_2 + jB_2 = (K_2 + jH_2)/K_1$  which corresponds to the junction admittance seen from the other side in Fig. 8. (Admittance is again used to simplify the explanation. For a coupler with series junctions, replace admittance, conductance and susceptance, by impedance, resistance and reactance, respectively.) It is obtained as indicated in Fig. 9 by first following the arrowed line along an "arg  $Y = \text{constant}$ " contour, down to the unit conductance circle, and thence following a constant susceptance contour as far as the circle  $Y = K_2/K_1$ . By stopping on this circle we ensure inverting the conductance component from  $K_1/K_2$  at the start to  $A_2 = K_2/K_1$ . That the susceptance component comes out as it should can be deduced from the fact that the lower portion of the arrowed path keeps the susceptance constant, by definition, while the upper portion follows an "arg  $Y = \text{constant}$ " contour, and therefore the real and imaginary parts of  $Y$  are multiplied up or down together. Now the real part changes from  $K_1/K_2$  to unity (following the arrow), and therefore the imaginary part is also multiplied by  $K_2/K_1$ , and this is just what is needed to turn  $jH_2/K_2$  into  $jH_2/K_1$ . Incidentally, the two points marked "START" and  $A_2 + jB_2$  are necessarily at the same radius, since the normalized junction reflection coefficient, or the junction VSWR, of a lossless junction is independent of which port is taken as the input side.

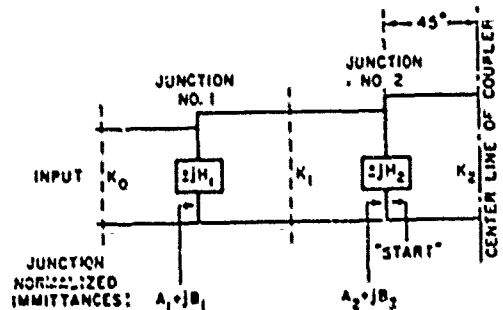


FIG. 8 EVEN-OR ODD-MODE EQUIVALENT CIRCUIT FOR DESIGN OF FOUR-BRANCH ( $n = 3$ ) COUPLER USED IN EXAMPLE III-1

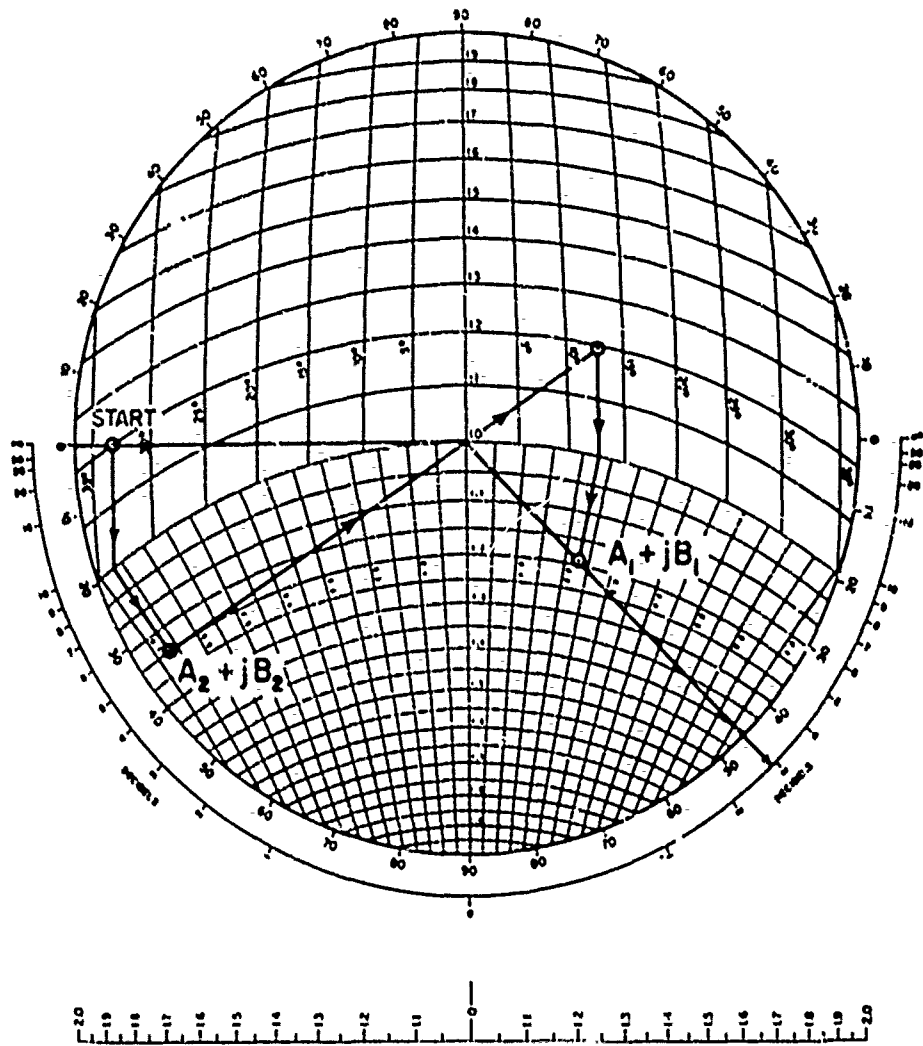


FIG. 9 SOLUTION BY CHART OF FOUR-BRANCH ( $n = 3$ ) COUPLER USED IN EXAMPLE III-1

To move on to junction 1, the restriction  $\phi_1'' = 90^\circ - \phi_2'$  determines the direction of the radius in Fig. 9. It points into the upper left-hand quadrant, and images the radius to  $A_2 + jB_2$  in the horizontal line. For construction purposes it is easier to ignore differences between left and right of the vertical center line, and simply to continue the radius from  $A_2 + jB_2$  along a straight line following the arrow into the upper right-hand quadrant in Fig. 9. The distance out to the circle there corresponds to a VSWR of  $V_1 = 1.311$ . On a full Smith chart this point would give the admittance in the plane of the first junction seen from the line  $K_1$ , i.e., the admittance  $(K_0 + jH_1)/K_1$ . By the same construction as before we now turn this admittance into  $A_1 + jB_1 = (K_1 + jH_1)/K_0$ , which is the admittance of the first junction seen from the line  $K_0$ . All the coupler admittances are now found as follows, normalized to  $K_0 = 1.0$ :

$$\begin{aligned} K_1 &= A_1 = 1.189 & H_1 &= B_1 = 0.228 \\ K_2 &= A_2 K_1 = 1.429 & H_2 &= B_2 K_1 = 0.7925 \end{aligned} \quad (5)$$

where  $B_1$  and  $B_2$  are simply taken as positive, since differences between the left and right half are being ignored. In general, the solution when the number of sections,  $n$ , is odd (when the number of branches,  $n + 1$ , is even) is obtained from:

$$\left. \begin{aligned} K_0 &= 1 \\ K_1 &= A_1 \\ K_2 &= A_1 A_2 \\ K_3 &= A_1 A_2 A_3 \\ K_4 &= A_1 A_2 A_3 A_4 \\ &\vdots \\ \text{etc., and} \\ H_1 &= B_1 \\ H_2 &= A_1 B_2 \\ H_3 &= A_1 A_2 B_3 \\ H_4 &= A_1 A_2 A_3 B_4 \end{aligned} \right\} \quad (6)$$

etc.

If the coupler consists of series instead of shunt junctions, then  $K$  and  $H$  are impedances instead of admittances.

The coupling coefficient at center frequency for a matched coupler can also be read off from Fig. 9, by extending the radius through  $(A_1 + jB_1)$  to the outermost scale. In this case it is 2.9 db. The coupling when the input is matched is given by the difference in phase shifts suffered by the even and odd modes. Now the phase shift between reference planes (with real  $\Gamma$ ) is a multiple of 90 degrees, and is the same for both modes. It is therefore necessary to calculate the separation between the even- and odd-mode reference planes at either end of the coupler. These separations are the same at the two ends of the coupler, by symmetry, and are in equal and opposite directions for the two modes from the position corresponding to no coupling. The coupling  $C$  (db) at center frequency (where the coupler is perfectly matched since  $n$  is odd) is finally found to be equal to the square of the sine of the angle between the radius to  $A_1 + jB_1$  and the horizontal axis. Expressed in decibels, it is marked off on the lower outer scale in Fig. 9. It is seen that for 0-db coupling (complete cross-over) to be possible, all of the points  $A_1 \pm jB_1$  would have to lie on the vertical axis. It will in fact be seen later [Eq. (11a)] that 0-db coupling with a single design becomes possible only in the limit of  $R$  tending to infinity. A 0-db coupler has therefore to be designed as two or more couplers in cascade, e.g. two 3-db couplers, or three 6-db couplers, etc.

*Example III-2—Case of  $n =$  even.* Design a branch-guide coupler based upon a quarter-wave transformer of  $n = 4$  sections, output-to-input impedance ratio  $R = 6$ , and bandwidth  $\omega_0 = 1.00$ .

From the tables<sup>12,13</sup> the junction VSWRs of the prototype transformer are  $V_1 = 1.247$ ,  $V_2 = 1.518$ ,  $V_3 = 1.672$ . Half the coupler for either the even or the odd mode is shown in Fig. 10. The third junction from the end is the middle junction, and the lines on either side of it have the same admittances,  $K_2$ . The junction admittance seen from either side is  $1 + jH_3/K_2$ ; its real part is thus unity, and it must correspond to a VSWR of  $V_3 = 1.672$ . This is the point marked "START" in Fig. 11, situated on the unit conductance circle. Apart from this different beginning, all subsequent steps are as in Example III-1, and it is found that:

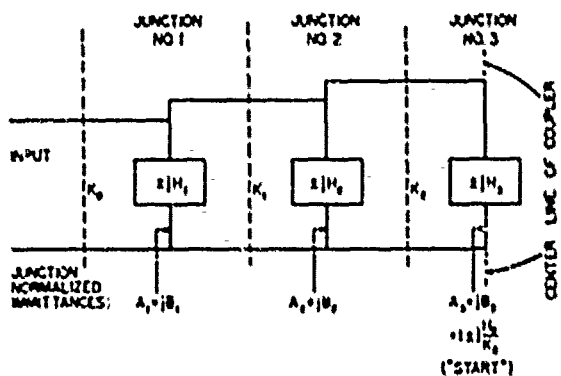


**FIG. 10 EVEN- OR ODD-MODE EQUIVALENT CIRCUIT FOR DESIGN OF FIVE-BRANCH ( $n = 4$ ) COUPLER USED IN EXAMPLE III-2**

$$\begin{aligned} K_0 &= 1.0 & H_1 &= B_1 = 0.180 \\ K_1 &= A_1 = 1.155 & H_2 &= B_2 K_1 = 0.481 \\ K_2 &= A_2 K_1 = 1.383 & H_3 &= B_3 K_2 = 0.719 \end{aligned} \quad (7)$$

The general solution is still given by Eq. (6). The coupling  $C$  (db) at center frequency (where this coupler has a very low VSWR) is read off as before and is again 2.9 db. It will be seen later [Eq. (11a)] that the coupling is only a function of  $R$ , when the reflection loss is negligible, and since  $R = 6$  in both examples, this result was to be expected. An expression for the actual coupling  $P_{2,1}$  (db) when there is appreciable reflection loss will also be given later [Eq. (11b)].

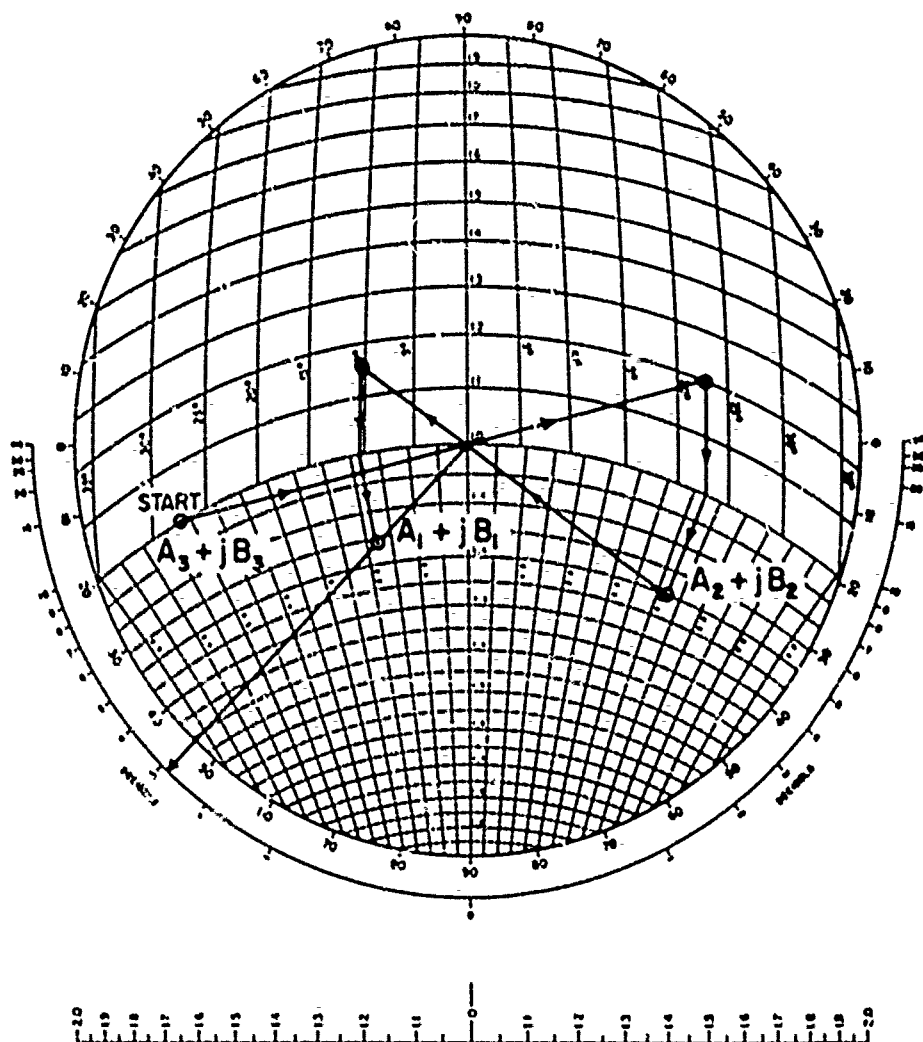


FIG. 11 SOLUTION BY CHART OF FIVE-BRANCH ( $n = 4$ ) COUPLER USED IN EXAMPLE III-2

#### IV CHOICE OF QUARTER-WAVE TRANSFORMER PROTOTYPE

The even- or odd-mode half of the branch-guide coupler has been modulated on the quarter-wave transformer at center-frequency. If the prototype transformer has a wide-band Tchebyscheff response, then the branch-guide coupler may similarly be expected to have low VSWR and high directivity over a wide band of frequencies; if the prototype transformer is narrow-band or maximally flat, then the branch-guide coupler VSWR and directivity response may be expected to be narrow-band or approximately maximally flat. The coupling from one line over to the other ( $P_2$ , on Fig. 2) is generally found to increase slowly as the frequency moves away from band center (either up or down), and is less obviously dependent on the prototype characteristics. One would like to have some criteria leading from the specification for the coupler to the selection of the prototype transformer that will transform it into a coupler meeting the specification.

Let  $V$  and  $\Gamma$  be the VSWR and associated reflection coefficient of the branch-guide coupler at any frequency; let  $V'$  and  $\Gamma'$  be the VSWR and associated reflection coefficient of the prototype quarter-wave transformer at the corresponding frequency. An examination of the phase relationships between reflected and transmitted waves<sup>14</sup> shows that, at center frequency,

$$\left. \begin{aligned} \Gamma &= \frac{1}{(1 - \Gamma'^2)^{1/2}} \cdot \frac{\Gamma'}{\text{antilog}(P_2/20)} \\ &= \frac{V + 1}{2V'} \frac{\Gamma'}{\text{antilog}(P_2/20)} \end{aligned} \right\} \quad (8a)$$

and the directivity<sup>15</sup>  $D$  in decibels is given by

<sup>14</sup>i.e., the output from the port immediately below the input port in Fig. 1 is  $(D + P_2)$  decibels below the input power.

$$D = -20 \log_{10} \left\{ \begin{aligned} & \left[ \frac{1}{(1 - \Gamma^2)^{1/2}} \frac{\Gamma'}{\text{antilog } (P_1/20)} \right] - P_2 \text{ db} \\ & -20 \log_{10} \left[ \frac{V + 1}{2V^{1/2}} \frac{\Gamma'}{\text{antilog } (P_1/20)} \right] - P_2 \text{ db} \end{aligned} \right\} \quad (9a)$$

Equations (8a) and (9a) also hold approximately near center frequency.

We shall now define a bandwidth contraction factor,  $\beta$ , as follows: If the prototype transformer fractional bandwidth is  $\nu_0$ , over which its VSWR does not exceed  $V'_{\text{max}}$  (the associated reflection coefficient being  $\Gamma'_{\text{max}}$ ), then the branch-guide coupler fractional bandwidth is  $\beta\nu_0$ , over which its VSWR does not exceed  $V'_{\text{max}}$  (the associated reflection coefficient being  $\Gamma'_{\text{max}}$ ), and its directivity is better than  $D_{\text{min}}$  decibels.

Equations (8a) and (9a) hold approximately when  $V_{\text{max}}$ ,  $V'_{\text{max}}$ ,  $\Gamma_{\text{max}}$ ,  $\Gamma'_{\text{max}}$ , and  $D_{\text{min}}$  are substituted for  $V$ ,  $V'$ ,  $\Gamma$ ,  $\Gamma'$ , and  $D$  respectively. In most cases,  $V'_{\text{max}}$  will be close to unity (i.e.,  $\Gamma'_{\text{max}}$  will be small compared to unity); neglecting  $\Gamma^2$  compared to unity, Eqs. (8a) and (9a) reduce to

$$\Gamma_{\text{max}} = \frac{\Gamma'_{\text{max}}}{\text{antilog } (P_1/20)} \quad (8b)$$

$$D_{\text{min}} = -20 \log_{10} \left[ \frac{\Gamma'_{\text{max}}}{\text{antilog } (P_1/20)} \right] - P_2 \quad (9b)$$

Making the additional convenient approximation when  $\Gamma$  is small, and  $\Gamma = (V - 1)/2$ ,

$$V_{\text{max}} = 1 + \frac{V'_{\text{max}} - 1}{\text{antilog } (P_1/20)} \quad (8c)$$

$$D_{\text{min}} = -20 \log_{10} \left[ \frac{V'_{\text{max}} - 1}{2 \text{antilog } (P_1/20)} \right] - P_2 \quad (9c)$$

One can combine Eqs. (8a) and (9a) to obtain, at center frequency (this becomes an approximation near center frequency),

$$\frac{10^{-(P_1+P_2)/20}}{1} = \frac{\text{antilog } (P_2/20)}{\text{antilog } (P_1/20)} \quad (10)$$

(Note—In Eqs. (8), (9), and (10)  $P_1$  and  $P_2$  are positive quantities and the antilogs are quantities greater than unity. For instance, for a 6-db coupler,  $P_2 = 6$  db, and  $\text{antilog } (P_2/20) = 2$ . If the coupler is also matched, then  $P_1 = 1.25$  db, and  $\text{antilog } (P_1/20) = 1.154$ .)

The ratios on either side of Eq. (10) are the same quantity as the ratio  $E_4/E_3 = X/Y$  in Ref. 3, and can be calculated from the formulas given there.

Equations (8), (9), and (10) apply to synchronous couplers, but not necessarily to others. For example, they do not generally apply to periodic couplers (Section VI).

When the coupler is matched at center frequency, then the coupling  $P_2$  at center frequency will be denoted by  $C$  (db). It can be related to  $R$  by the formula

$$C = 20 \log_{10} \left( \frac{R+1}{R-1} \right) \text{ db} \quad (11a)$$

in all the numerical solutions attempted. A general proof for this formula has not yet been found. The coupling  $C$  does not depend on the number of branches or the bandwidth. The relation between  $C$  and  $R$  is graphed in Fig. 12, and a few more common values are tabulated in Table 1. When the coupler is not matched at center frequency, and

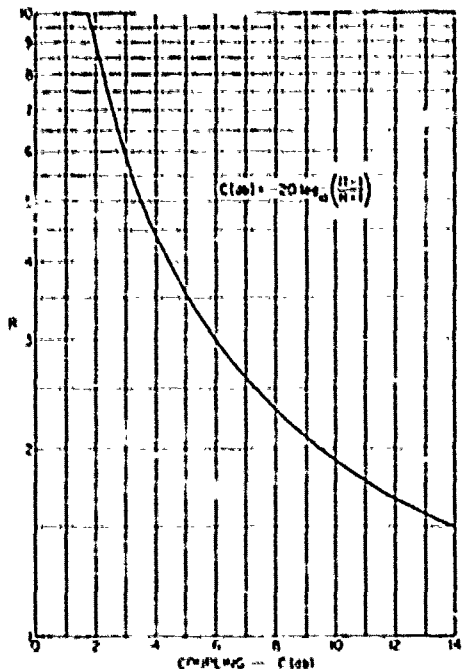


FIG. 12 PLOT OF CENTER FREQUENCY COUPLING  $C$  (db) vs. IMPEDANCE RATIO PARAMETER,  $R$ , FOR A MATCHED COUPLER

its prototype transformer has a VSWR  $V_0'$  at center frequency, then the center frequency coupling  $P_{2,0}$  is given by

$$P_{2,0} = C - 10 \log_{10} \left[ \frac{(V_0' + 1)^2}{4V_0'} \right] \text{ dB} \quad (11b)$$

at least for every coupler given in the tables in Appendix I.

The branch-guide coupler characteristics (like those of the prototype transformer) will be symmetrical about the center frequency when plotted against  $\lambda_{g0}/\lambda_g$ , where  $\lambda_g$  is any guide wavelength, and  $\lambda_{g0}$  is the particular guide wavelength at band-center, defined as follows. Let  $\lambda_{g1}$  and  $\lambda_{g2}$  be the longest and shortest guide wavelengths in the pass band; then  $\lambda_{g0}$  is defined by

$$\lambda_{g0} = \frac{2\lambda_{g1}\lambda_{g2}}{\lambda_{g1} + \lambda_{g2}} \quad . \quad (12a)$$

The fractional bandwidth of the branch-guide coupler will be denoted by  $\nu_b$  and is defined (analogously to the quarter-wave transformer fractional bandwidth,  $\nu_q$ ) by

$$\nu_b = 2 \left( \frac{\lambda_{g1} - \lambda_{g2}}{\lambda_{g1} + \lambda_{g2}} \right) \quad . \quad (12b)$$

It has been found that the coupler fractional bandwidth  $\nu_b$  is always less than the prototype transformer fractional bandwidth  $\nu_q$ . Their ratio is denoted by

$$\beta = \frac{\nu_b}{\nu_q} \quad . \quad (13)$$

which is the bandwidth contraction factor already referred to.

Before we can select the appropriate quarter-wave transformer prototype from which to derive our branch-guide coupler, we have to

TABLE I  
TABLE CONNECTING THE IMPEDANCE  
RATIO PARAMETER R WITH THE  
COUPLING C (dB) AT CENTER  
FREQUENCY FOR A  
MATCHED COUPLER

R	C (dB)	C (dB)	R
1.25	19.06	20	1.222
1.5	13.97	17	1.330
2.0	9.54	15	1.432
2.5	7.35	14	1.498
3.0	6.02	10	1.925
4.0	4.63	7	2.617
5.0	3.52	6	3.012
6.0	2.92	4	4.412
8.0	2.18	3	5.84
10.0	1.74	1	17.41

know the bandwidth contraction factor,  $\beta$ . An examination of a large number of cases from maximally flat prototypes to prototypes having bandwidths of at least 80 percent, showed that the bandwidth contraction factor  $\beta$  did not change appreciably with bandwidth, but did change with the number of sections  $n$  (number of branches  $\approx n+1$ ), and the impedance-ratio parameter  $K$ . Because predicting  $\beta$  from the T-junction properties seemed too formidable an undertaking, a large number of branch-guide couplers were analyzed and their bandwidths compared to those of their prototype transformers. From this comparison the graph of Fig. 13 was prepared. The bandwidth contraction factor  $\beta$  was found to lie between 0.5 and 0.7 in most cases; it was nearer the upper value of 0.7 for weaker couplings (smaller  $R$ ) and fewer sections (lower  $n$ ). An example of the use of Fig. 13 in the selection of a prototype will now be given.

**Example IV-1—Design of a 3-db Coupler.** Find the prototype transformer for a 3-db branch-guide coupler which is to have an input VSWR

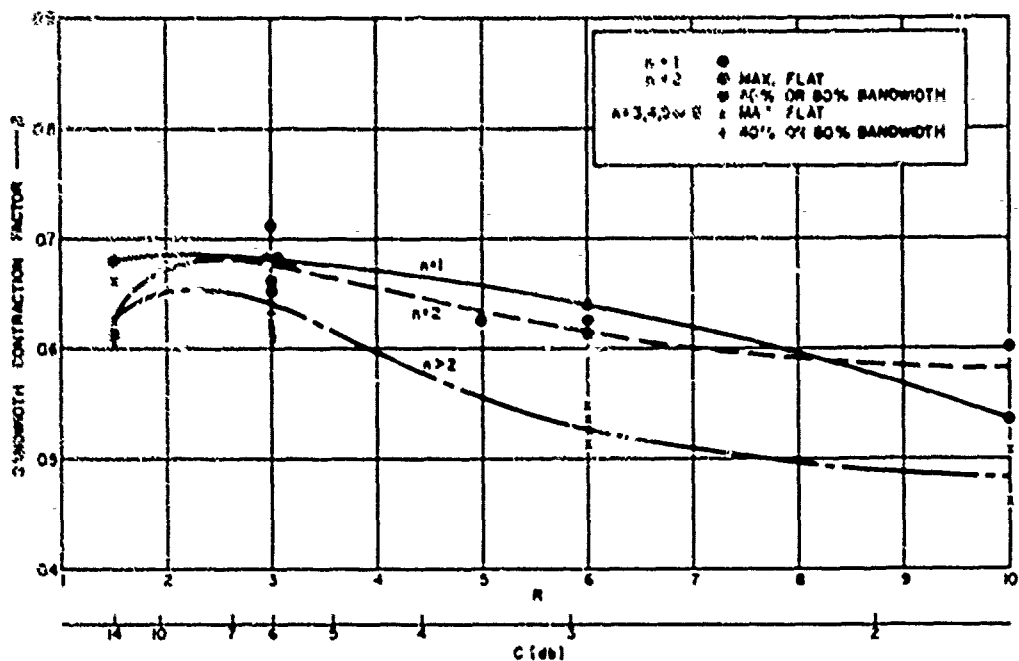


FIG. 13 BEST ESTIMATES FOR BANDWIDTH CONTRACTION FACTOR,  $\beta$ , BASED ON 27 INDIVIDUAL SOLUTIONS

below 1.10 and directivity in excess of 20 db over a 24-percent fractional bandwidth.

From Fig. 12 or Table I, when  $G = 3$  db, then  $R = 5.34$ . Try a two-branch coupler first, corresponding to a single-section quarter-wave transformer ( $n = 1$ ). From Fig. 13,  $\beta = 0.64$  for  $n = 1$ , so that the prototype fractional bandwidth must be  $\omega_c/\beta = 24/0.64$  percent, or nearly 40 percent by Eq. (13). The maximum VSWR of a single-section quarter-wave transformer<sup>12</sup> of  $R = 6$  and  $\omega_c = 0.40$ , is 1.860. It follows from Eq. (8b) that  $V_{max}$  of the coupler would then be considerably greater than the 1.10 specified.

Try a three-branch coupler next, corresponding to a two-section quarter-wave transformer ( $n = 2$ ). From Fig. 13,  $\beta = 0.62$  for  $n = 2$ , so that the prototype fractional bandwidth must be 24/0.62 percent, or almost 40 percent. Now the maximum VSWR of a two-section quarter-wave transformer<sup>12</sup> of  $R = 6$ ,  $\omega_c = 0.40$ , is 1.11, which for a 3-db coupler by Eq. (8c) yields  $V_{max} = 1 + 0.11/1.414 = 1.08$  which is below the 1.10 specified. The directivity from Eq. (9b) or (9c) will be better than  $-20 \log_{10} (0.04) - P_1 = 25$  db which exceeds the 20 db specified.

Thus the prototype quarter-wave transformer will in this case have two sections ( $n = 2$ ),  $R = 5.84$ , and bandwidth  $\omega_c = 0.40$ . Its junction VSWRs can be found from tables,<sup>12</sup> and then converted to the branch-guide coupler parameters either by means of charts (see Examples III-1 and III-2 of the last section) or by interpolating from the tables in Appendix A.

Nothing has yet been said about the variation of the couplings  $P_1$  and  $P_2$  with frequency. This is analogous to prescribing the amplitude characteristic of a filter and then asking about its phase (or time-delay) characteristic. The amplitude and phase characteristics are related and cannot be prescribed independently of each other. In the case of the branch-guide coupler the coupling characteristics are determined by the difference between the even- and odd-mode phase characteristics. To obtain a systematic picture of the frequency variation of the VSWR  $V$ , the directivity  $D$  (db) and the two couplings (the in-line coupling  $P_1$  and the cross-over coupling  $P_2$ , both in db), these were plotted in Figs. 14, 15, and 16 for couplers based on maximally flat quarter-wave transformer prototypes for  $n = 1, 2, 4$ , and 8, and for  $R = 1.5, 3$ , and 6, corresponding to couplings ( $G$ ) of approximately 14, 6 and 3 db (Table I). The graphs are plotted against the quantity  $(\lambda_{g0}/\lambda_g)$ , where

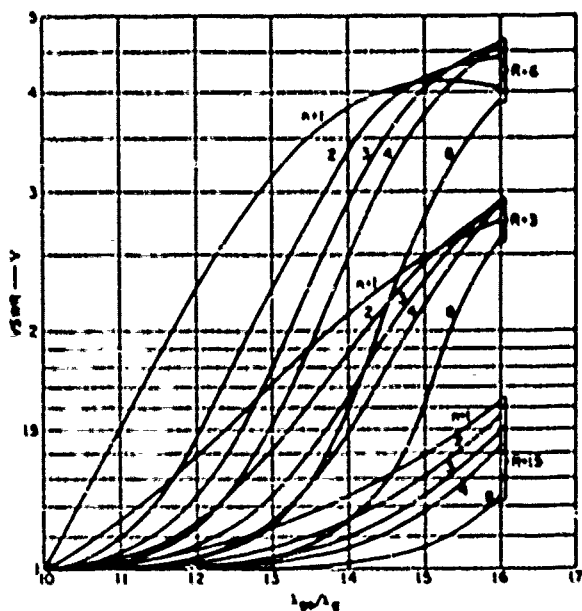


FIG. 14 VSWR CHARACTERISTICS OF SOME MAXIMALLY FLAT COUPLERS (Immittances of these couplers are given in Tables I-1 and I-2 of Appendix I)

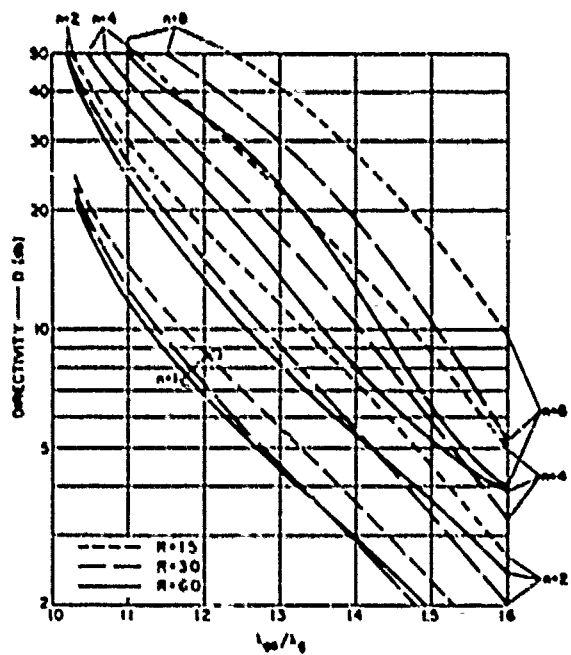


FIG. 13 DIRECTIVITY CHARACTERISTICS OF SOME MAXIMALLY FLAT COUPLERS (Immittances of these couplers are given in Tables I-1 and I-2 of Appendix I)

$\lambda_g$  is the guide wavelength, and  $\lambda_{g0}$  is its value at band-center [Eq. (12a)]. The response is symmetrical about  $(\lambda_{g0}/\lambda_g) = 1$ , so that Figs. 14, 15, and 16 actually cover the range from 0.4 to 1.6, although only the portion from 1.0 to 1.6 is shown. For non-dispersive (TEM mode) lines, the guide wavelength  $\lambda_g$  reduces to the free space wavelength  $\lambda$ , and then  $\lambda_{g0}/\lambda_g$  reduces to  $\lambda_0/\lambda = f/f_0$ , where  $f$  is the frequency, and  $f_0$  is its value at band-center (also called the center frequency).

It can be seen from Fig. 16 that the coupling  $P_2$  generally becomes stronger ( $P_2$  measured in decibels decreases) on either side of center frequency (the curves are symmetrical about  $\lambda_{g0}/\lambda_g = 1$ ), and correspondingly  $P_1$  becomes weaker ( $P_1$  measured in decibels increases).

Now return to Example IV-1. If we may use Fig. 16 as a guide, then over the 24-percent band specified this three-branch 3-db coupler would be expected to change each of its couplings,  $P_1$  and  $P_2$ , by a little under 0.3 db. Thus if the coupler were designed to have 3-db coupling at center frequency (corresponding to  $R = 5.84$  picked before), then  $P_2$  would go to 2.7 db and  $P_1$  to 3.3 db at the 24-percent band edges. If the specification asked for both  $P_1$  and  $P_2$  to be maintained to within  $\pm 0.15$  db of 3 db over the 24-percent band, or generally to optimize the balance over the band as a whole, then the coupler would be designed with  $P_{2,0} = 3.15$  db, corresponding to  $R = 5.7$ , by Fig. 12 or Eq. (11a). This coupler was designed (using the tables in Appendix A) and has the following parameters:

$$K_0 = 1, \quad K_1 = 1.2902, \quad H_1 = 0.4363, \quad H_2 = 1.0844.$$

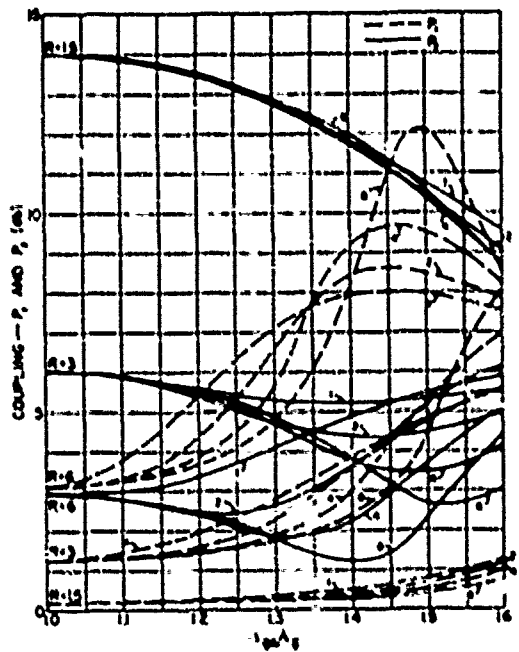


FIG. 16 COUPLING CHARACTERISTICS OF SOME MAXIMALLY FLAT COUPLERS (Immittances of these couplers are given in Tables I-1 and I-2 of Appendix I)

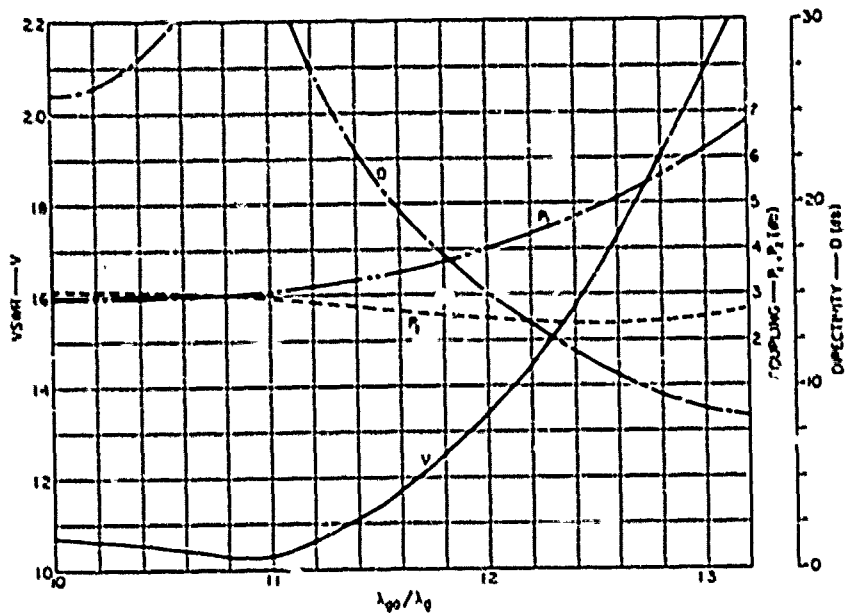


FIG. 17 COMPUTED PERFORMANCE OF THREE-BRANCH ( $n = 2$ ) COUPLER OF EXAMPLE IV-1

Its analyzed performance is reproduced in Fig. 17, and it is found to conform very closely to the specifications. (Again, this is plotted only for one side of band-center, since the response is symmetrical as plotted.) From Fig. 17, the analyzed performance over the 24-percent bandwidth is: Maximum VSWR, 1.07 (1.08 was predicted); Minimum directivity, 26 db (25 db was predicted); Couplings  $P_1$  and  $P_2$ , both within  $\pm 0.2$  db of 3 db ( $\pm 0.15$  db was predicted).

## V FURTHER NUMERICAL EXAMPLES

In applying any approximate design procedure, the question inevitably arises: How accurate is it? One way to answer this question is to analyze numerically the performance of some representative cases. A few more of these sample cases which were analyzed are reproduced in this section.

*Example V-1—Design of a 6-db Coupler.* Optimize a five-branch 6-db coupler over a 25-percent fractional bandwidth. Estimate the maximum VSWR and the minimum directivity over this band, and the variation in coupling.

For a well-matched coupler, a coupling coefficient of 6 db requires  $R = 3$ , by Table I. The bandwidth contraction factor,  $\beta$ , is 0.64 from Fig. 13. For a coupler fractional bandwidth  $\omega_b = 25$  percent, we therefore require  $\omega_b = 0.25/0.64 = 0.4$ . From data on quarter-wave transformers for  $n = 4$  (Table III of Ref. 12) the maximum passband VSWR ( $V'_{max}$ ) for the quarter-wave transformer will be less than 1.01. Therefore  $V_{max}$  will be less than 1.005 for the branch-guide coupler, by Eq. (8c), since  $P_1 = 6$  db. The directivity by Eq. (9c) should be better than  $-20 \log_{10} (0.005/2 \times 0.866) = 6 = 44$  db, since  $P_1 = 1.25$  db for a well-matched 6-db branch-guide coupler.

This coupler was designed by chart, and then constructed in waveguide according to the impedance values so obtained. The impedances were later recomputed more accurately from the tables in Appendix I after the coupler had already been built. (These later and more accurate values are shown in brackets below, as they were not used in constructing the coupler.) It was found that

$$\left. \begin{array}{ll}
 K_0 = 1.0 \text{ (1.0)} & H_1 = 0.070 \text{ (0.0688)} \\
 K_1 = 1.036 \text{ (1.0367)} & H_2 = 0.274 \text{ (0.2823)} \\
 K_2 = 1.127 \text{ (1.1323)} & H_3 = 0.450 \text{ (0.4522)}
 \end{array} \right\} \quad (14)$$

A comparison between the first set of numbers (calculated by chart) and the numbers in brackets (calculated by digital computer) gives an indication of the accuracy obtainable by chart. Here it is about 2 percent in  $H$  and in  $(K - 1)$  on the average.\*

The analyzed performance of the coupler with the impedances in brackets (obtained by digital computer) conforms very closely to the predicted values of maximum VSWR and minimum directivity over the 25-percent pass band: its computed values by analysis were respectively 1.005 for the maximum VSWR (compare 1.005 predicted), and 43 db for the minimum directivity (compare 44 db predicted); the center frequency coupling is exactly 6.02 db. The analyzed performance of the coupler with the first set of impedances (obtained by chart) is little changed though the maximum VSWR in the 25-percent pass band is now 1.01, and the minimum directivity 34 db; the center frequency coupling is 6.1 db. Junction discontinuity effects and mechanical tolerances may be expected to have a greater effect on performance than inaccuracies due to using the chart; it may therefore be concluded that the charts are almost as accurate as the tables for most practical purposes.

The analyzed performance of the coupler (designed by chart) is shown in Fig. 18, together with the experimental results in waveguide, which will be described later.

The variation in coupling may be estimated from Fig. 16. It is seen from the curve for  $n = 4$ ,  $R = 3$ , that  $P_2$  changes from 6 db at band-center by 0.2 db to 5.8 db at the 25-percent band-edges ( $\lambda_{g0}/\lambda_g = 1 \pm 0.125$ ). The analyzed performance (Fig. 18) shows a like change of about 0.2 db from band-center (6.1 db) to band-edges (5.9 db).

*Example V-2—Design of a 0-db Coupler.* Design a thirteen-branch 0-db coupler making use of the five-branch coupler ( $n = 4$ ) of the previous example. What maximum insertion loss would one expect over a 40-percent fractional bandwidth?

The 0-db coupler can be put together from three 6-db couplers, as follows from Appendix B. By merging the end branches of adjacent couplers, two branches can be eliminated, and the 0-db coupler has thus thirteen branches. Its immittances, based on Eq. (14), are as follows:

\* This was one of several early examples worked out quickly on the charts. With a little more care, the accuracy is about 1 percent. Compare Example V-4.

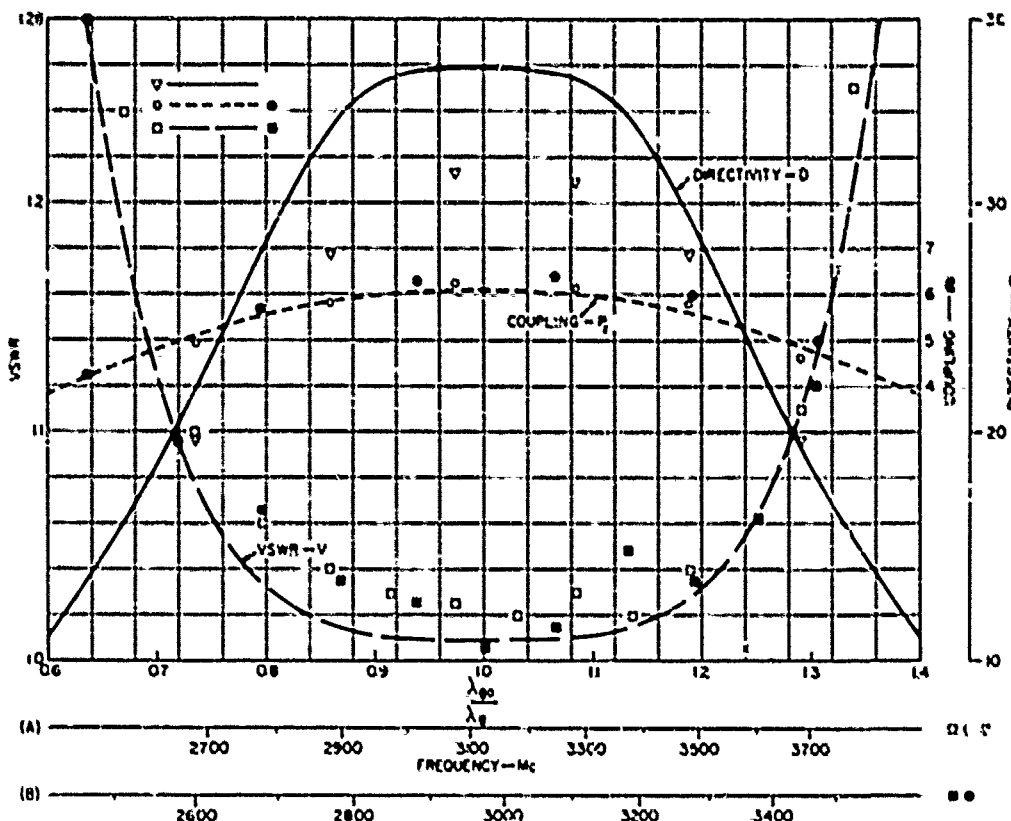


FIG. 18 PERFORMANCE OF FIVE-BRANCH ( $n = 4$ ) COUPLER OF EXAMPLE IV-1  
(Lines are computed; points are measured on experimental models shown in  
Figs. 27, 28, and 29)

$$\begin{aligned}
K_0 &= K_{13} = 1.0 \\
K_1 &= K_4 = K_5 = K_8 = K_9 = K_{12} = 1.036 \\
K_2 &= K_3 = K_6 = K_7 = K_{10} = K_{11} = 1.127 \\
H_1 &= H_{13} = 0.070 \\
H_2 &= H_4 = H_6 = H_8 = H_{10} = H_{12} = 0.274 \\
H_3 &= H_5 = H_{11} = 0.450 \\
H_9 &= H_9 = 0.140
\end{aligned} \quad (15)$$

The coupler of Example V-1 varied in coupling from 6.1 db at band-center to 5.5 db over a 40-percent fractional bandwidth ( $\lambda_{wg}/\lambda_g$  from 0.6 to 1.2), as can be seen from Fig. 18. To work out the greatest deviation from 0 db of the new coupler we see from Appendix II that 5.5 db corresponds to a phase shift  $\theta$  in either the even or the odd mode of

$$\theta = \pm \text{arc sin} \left[ \text{antilog} \left( \frac{-5.5}{20} \right) \right] = \pm 32^\circ 4' \quad (16)$$

For the three couplers in cascade the combined phase shift in either mode will be approximately  $3\theta = \pm 96^\circ 12'$ , which corresponds to a coupling of

$$-20 \log_{10} (\sin 96^\circ 12') = 0.05 \text{ db} \quad (17)$$

This represents the maximum insertion loss, since the deviation from 0 db at band-center is even less. The performance of this coupler is shown in Figs. 19 and 20, together with the experimental results in waveguide, which will be described later. It is seen that the insertion loss upon analysis is indeed better than 0.05 db over a 40-percent fractional bandwidth. (The experimentally measured points also agree very closely.)

*Example V-3—A Coupler with  $3\lambda/4$  Branches.* It is required to lengthen the branches of the coupler in Example V-2 from one-quarter wavelength to three-quarters wavelength. The spacing between branches is to be kept one-quarter wavelength. It is to be determined how this affects the performance.

There is no way to predict accurately the reduction in bandwidth to be expected. If both the branch lengths and their spacings were tripled

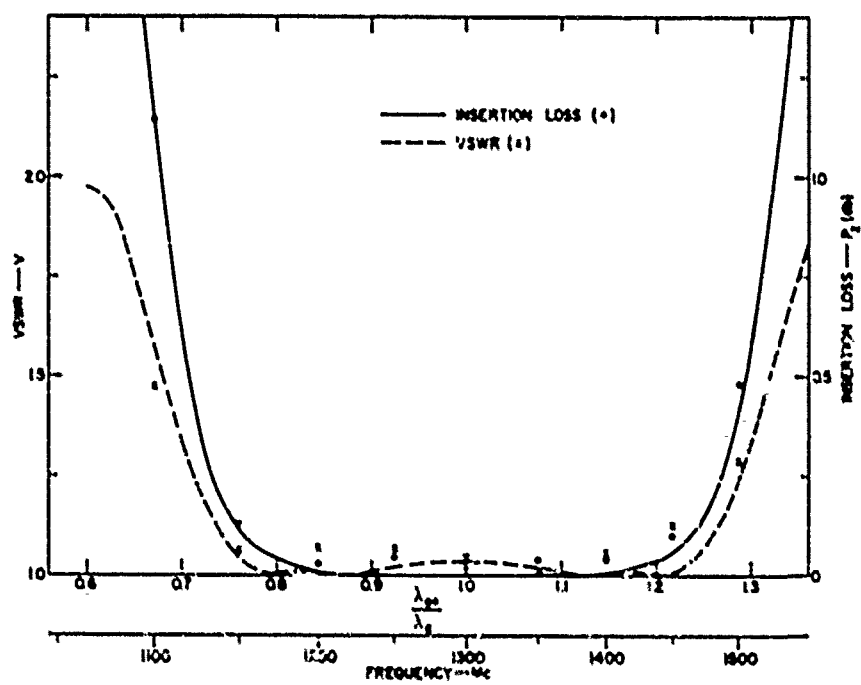


FIG. .9 INSERTION LOSS  $P_2$  (db) AND VSWR OF 0-db COUPLER (Fig. EXAMPLE V-2)  
 (Lines are computed; points are measured on experimental model shown in  
 Figs. 30 and 31)

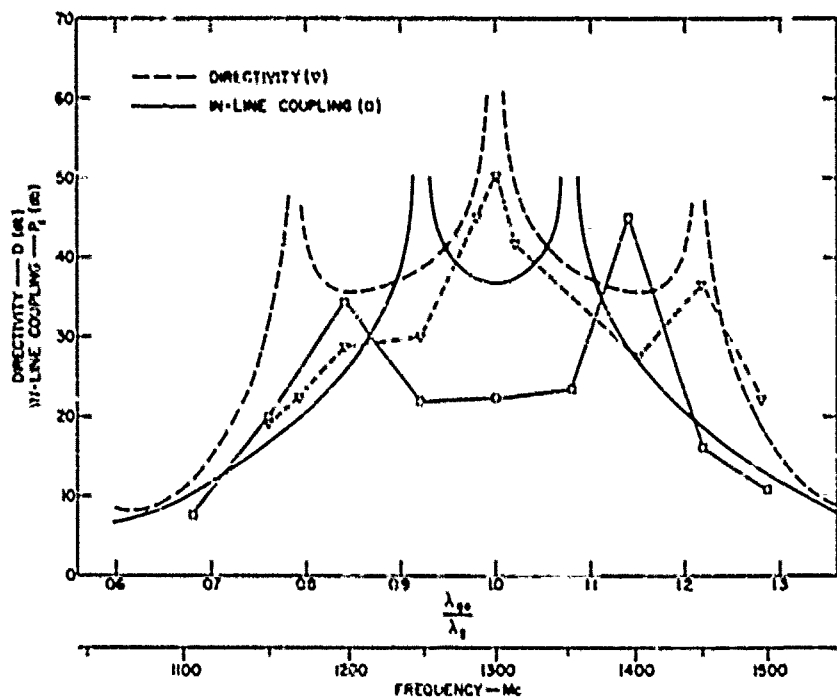


FIG. 20 DIRECTIVITY D AND IN-LINE COUPLING  $P_1$  OF 0-db COUPLER OF EXAMPLE V-2  
 (Lines are computed; points are measured on experimental model, Figs. 30 and 31)

together, the resulting bandwidth would be reduced to one-third, without otherwise affecting VSWR, coupling, etc. Since the branches are to be lengthened but not their spacings, we might expect a lesser reduction in bandwidth. This is borne out by the analysis. The VSWR and insertion loss of this coupler are plotted in Fig. 21. The insertion-loss bandwidth is reduced down to almost one-third of the original bandwidth (compare Figs. 19 and 21), but the VSWR bandwidth is less affected, and is reduced to only about one-half.

**Example V-4—A Three-Branch Coupler.** Consider a branch-guide coupler based on the following quarter-wave transformer prototype parameters:

$$\begin{aligned}n &= 2 \\R &= 5.0 \\w_1 &= 0.8\end{aligned}$$

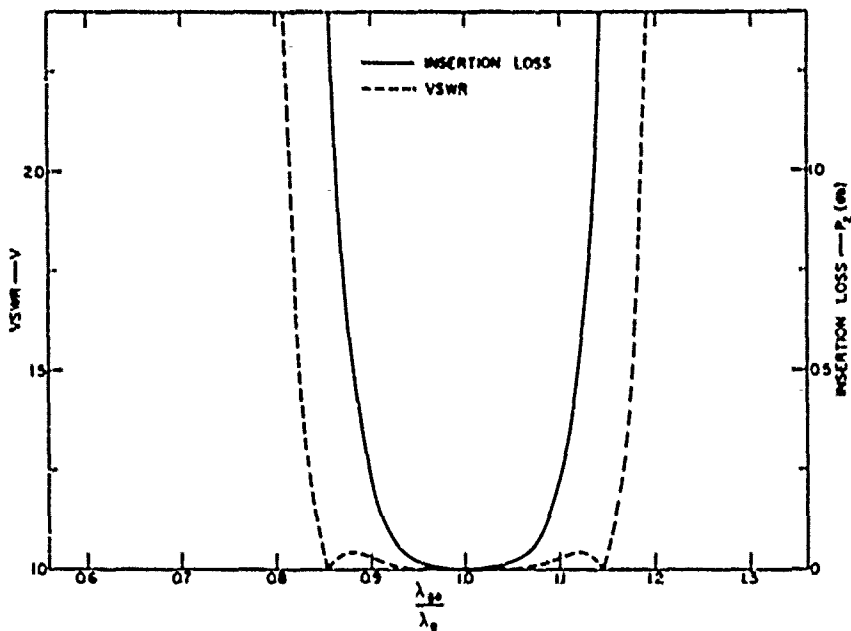


FIG. 21 COMPUTED PERFORMANCE OF 0-db COUPLER WITH BRANCHES  $3\lambda/4$  LONG (Exam. 1e V-3)

Predict the coupler's maximum VSWR and minimum directivity over its pass band, and find its fractional bandwidth. Predict the maximum and minimum values of the two couplings  $P_1$  and  $P_2$  over the pass band. Finally, calculate the immittances  $K_1$ ,  $H_1$  and  $H_2$  of this coupler.

The maximum pass-band VSWR  $V_{max}^2$  of a quarter-wave transformer having  $n = 2$ ,  $R = 5$ ,  $w_0 = 0.80$  is, by Ref. 12, equal to 1.45. Therefore, the maximum VSWR ( $V_{max}$ ) of the coupler over its pass band is, according to Eq. (8c), approximately equal to

$$1 + \frac{0.45}{1.5} = 1.3 . \quad (18)$$

since  $R = 5$  corresponds to  $P_2 = 3.52$  db when the effect of mismatch is neglected. Since the VSWR has a maximum at band-center, because  $n$  is even, and this is equal to 1.45 for the prototype transformer (corresponding to a loss by reflection of 0.15 db), the coupling  $P_1$  is, by Eq. (11b), equal to 3.67 db.

Similarly from Eq. (9c), the directivity would be expected to be better than

$$-20 \log_{10} \left[ \frac{0.45}{2.82} \right] = 3.5 = 12.5 \text{ db} \quad (19)$$

over the pass band, where  $P_1$  has been set equal to 3 db for the moment. A more accurate estimate of  $P_1$  can now be made by balancing the input and output powers:

Coupled power (corresp. to 3.67 db)	=	0.430
Reflected power (corresp. to VSWR = 1.3)	=	0.017
Power in directivity arm (corresp. to 12.5 + 3.6 = 16.1 db)	=	0.025
		_____
Total so far	=	0.472

Hence the fraction of power out of the "in-line" arm is 0.528 (corresponding to  $P_1$  equal to 2.77 db). When this is substituted into Eq. (9c), then instead of Eq. (19) we obtain 13.6 db for the directivity. Making a new more accurate balance-sheet for the powers then gives

$$P_1 = 2.7 \text{ db} . \quad (20)$$

The coupler fractional bandwidth,  $\nu_1$ , predicted from Fig. 13 is  $0.80\beta = 0.80 \times 0.54 = 0.43$ .

Using Fig. 16 as a guide, we would expect  $P_2$  to change by about 0.67 db from 3.67 to about 3.0 db, and  $P_1$  by about 1.1 db from 2.7 to 3.8 db over the 43-percent band.

The immittance parameters of this coupler were obtained by chart. (They can also be read from the tables in Appendix I, and these immittances are shown in parentheses; they were not used in the subsequent analysis.)

$$K_0 = 1.0$$

$$K_1 = 1.29 \quad (1.2798)$$

$$H_1 = 0.50 \quad (0.4919)$$

$$H_2 = 0.812 \quad (0.8049)$$

Here the parameters obtained by chart and by computer agree to within one percent on the average.

This coupler (designed by chart) was analyzed, and its performance is plotted in Fig. 22. (Its response is symmetrical about  $\lambda_{g0}/\lambda_0 = 1.0$ , as usual.) Its analyzed and predicted performance agree closely. Over the 43-percent bandwidth, the maximum VSWR is 1.29 (the predicted VSWR was 1.3); its minimum directivity is 13.4 db (13.6 db was predicted); the coupling  $P_2$  changes from 3.65 to 2.7 db (3.67 to 3.0 db was predicted); and  $P_1$  changes from 2.7 to 3.4 db (2.7 to 3.8 db was predicted).

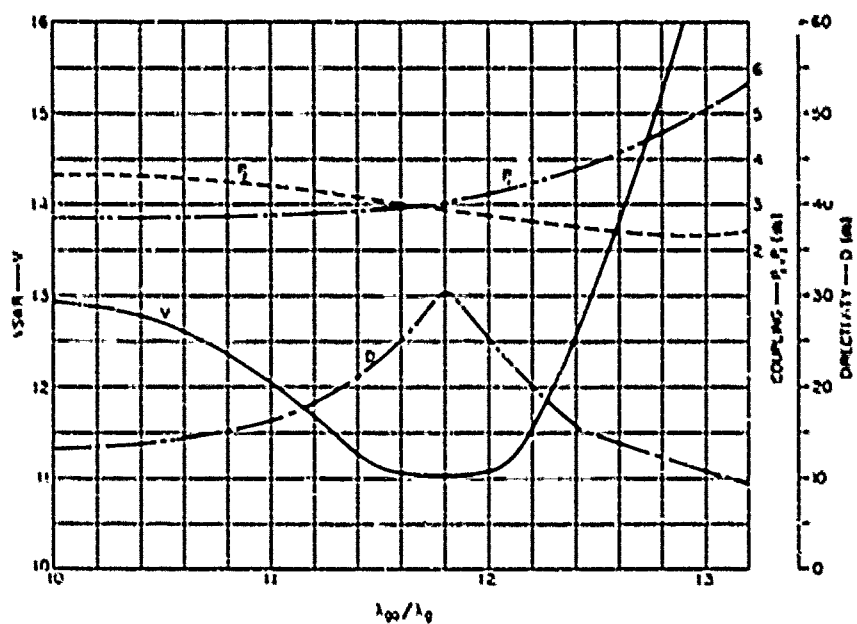


FIG. 22 COMPUTED PERFORMANCE OF THREE-BRANCH ( $n = 2$ ) COUPLER  
OF EXAMPLE V-4

## VI PERIODIC AND SYNCHRONOUS COUPLERS

Reed<sup>4</sup> has analyzed a class of branch-guide couplers in which the main line impedances are constant and equal to the input and output line impedances, and in which all the internal branches have the same impedance. These couplers will herein be referred to as "periodic couplers." They do not have a clearly defined pass band, over which the performance is optimized in some sense. Reed has given numerous curves for 0-db couplers and some for other coupling ratios, which may be used as a guide in some cases.

Couplers whose design is based on a quarter-wave transformer prototype are referred to as synchronous couplers (Section II). The performance of periodic and synchronous couplers will here be illustrated by examples. It may be stated as a rough guide that to achieve the same performance over a specified bandwidth, a periodic coupler requires about twice as many branches as a synchronous coupler.

Some suggestions to improve the performance of periodic couplers are also made, and illustrated by examples.

*Example VI-1—Comparison of Some 0-db Couplers.* Figures 23 and 24 show the VSWR-against-frequency and coupling-against-frequency characteristics of four 0-db couplers. Two of them are synchronously derived couplers, and two are periodic couplers.

Curve A is for the thirteen-branch 0-db coupler of Example V-2, except that the exact immittances  $K_i$  and  $H_i$  from the tables were used. [It is again based on three 6-db couplers with  $n = 4$ ,  $w_g = 0.40$ ,  $R = 3$ . The immittances this time come from the numbers shown in parentheses in Eq. (14), whereas previously Eq. (15) of Example V-2 was derived from the numbers obtained by chart " shown without parentheses in Eq. (14).]

Curve B is for a similar thirteen-branch 0-db coupler, differing from the previous one only in that it is based on a prototype transformer having  $w_g = 0.80$  (instead of 0.40). Curve C is Reed's<sup>4</sup> periodic coupler with thirteen branches. Curve D is Reed's<sup>4</sup> periodic coupler with twelve branches.

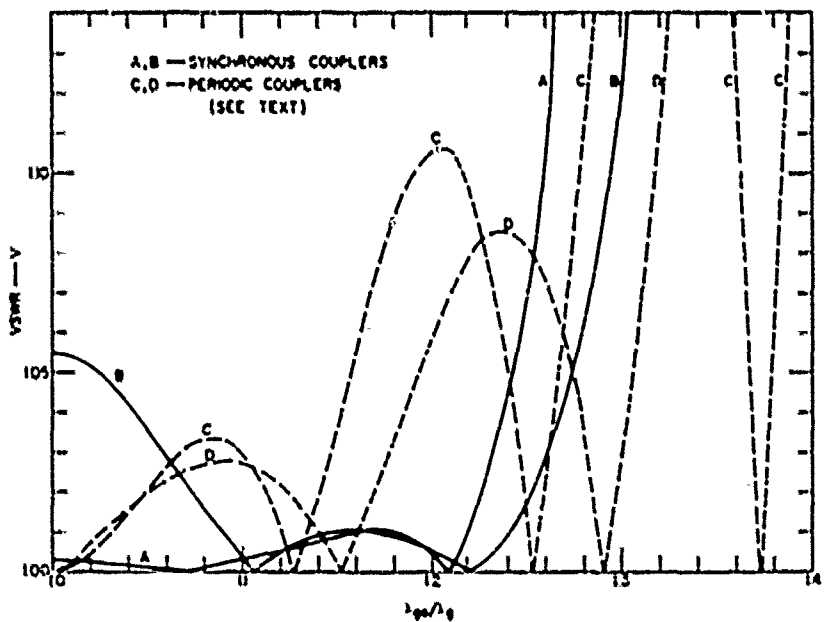


FIG. 23 VSWR CHARACTERISTICS OF FOUR 0-db COUPLERS  
 (Couplers A and B are synchronously derived, and  
 Couplers C and D are periodic as in Example VI-1)

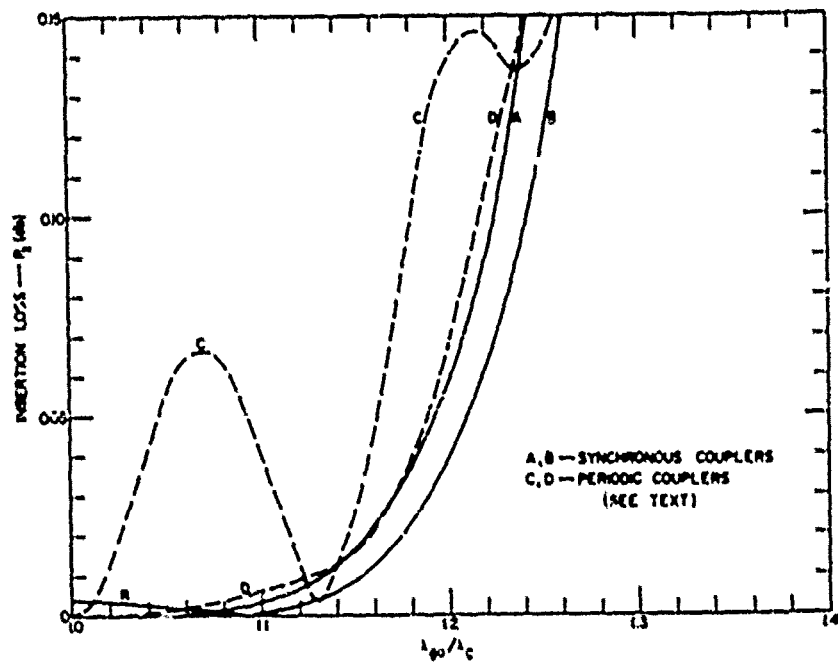


FIG. 24 INSERTION LOSS CHARACTERISTICS OF FOUR 0-dB COUPLERS  
 (Couples A and B are synchronously derived, and Couples C and D are periodic as in Example VI-1)

It is evident that Coupler C is inferior to the other three. This is typical of periodic couplers with an odd number of branches, and is due to the lack of matching end-branches. (Periodic couplers with an odd number of branches have all branch immittances the same, including the end branches.)

Coupler D is only slightly inferior to Coupler A as regards coupling  $P_2$ , but distinctly inferior as regards VSWR. Coupler B is similar to Coupler A, except that its peak VSWR at center frequency is higher, and it has a greater bandwidth.

The VSWRs of the two periodic couplers, Couplers C and D, exhibit ripples of increasing amplitude as the frequency deviation from band-center increases. There is no reflection at band-center, and there are zeros of reflection whenever the separation between end-branches increases or decreases by approximately one-half guide wavelength (Fig. 23). The couplings of the periodic couplers also exhibit similar periodic ripples (Fig. 24).

The VSWR and coupling of the two synchronously derived couplers, Couplers A and B, tend to remain constant in a fairly well defined pass band, outside which the curves rise steadily.

Since periodic couplers with an even number of branches are better than those with an odd number of branches, five couplers having 6, 8, 10, 12, and 14 branches were analyzed. Their performance was compared with three 7-branch, 0-dB couplers, which were "synchronously derived." This means that each 7-branch band-pass coupler was based on two identical, synchronous, 4-branch couplers (with  $R = 5.5$ ) placed in cascade, the two end-branches being merged. Three such couplers were designed and analyzed, and each was made optimum over a different bandwidth: they will be referred to as Case I, Case II, and Case III. They correspond to values of the prototype fractional bandwidth  $w$ , of 0.40, 0.60, and 0.80, respectively. Their immittances can be obtained readily from the tables in Appendix I, and are as shown in Table II.

Instead of plotting all of the curves for the five periodic couplers and the three synchronously derived couplers, the principal results are summarized in Tables III and IV.

TABLE II  
IMMITTANCES OF THREE SYNCHRONOUSLY DERIVED 0-<sup>1</sup>b COUPLERS

IMMITTANCES	CASE I	CASE II	CASE III
$K_0 = K_7$	1.0	1.0	1.0
$K_1 = K_3 = K_4 = K_6$	1.1563	1.1715	1.1951
$K_2 = K_5$	1.3852	1.3852	1.3852
$H_0 = H_6$	0.1957	0.2192	0.2500
$H_1 = H_2 = H_4 = H_5$	0.7618	0.7382	0.6995
$H_3$	0.3914	0.4384	0.5160

TABLE III  
MAXIMUM VSWR OF SEVERAL 0-db COUPLERS OVER STATED BANDWIDTHS

BANDWIDTH (percent)	PERIODIC COUPLERS					SEVEN-BRANCH SYNCHRONOUSLY DERIVED COUPLERS
	Six- branch	Eight- branch	Ten- branch	Twelve- branch	Fourteen- branch	
16	1.10	1.06	1.04	1.03	<u>1.02</u>	Case I 1.02
28	1.19	1.09	1.05	1.03	<u>1.02</u>	Case II 1.02
48	1.21	<u>1.10</u>	1.12	<u>1.09</u>	1.05	Case III 1.10

TABLE IV  
MAXIMUM INSERTION LOSS (db) OF SEVERAL  
0-db COUPLERS OVER STATED BANDWIDTHS

BANDWIDTH (percent)	PERIODIC COUPLERS					SEVEN-BRANCH SYNCHRONOUSLY DERIVED COUPLERS
	Six- branch	Eight- branch	Ten- branch	Twelve- branch	Fourteen- branch	
16	0.02	<u>0.01</u>	<u>0.006</u>	0.004	0.003	Case I 0.006
28	0.11	0.04	0.02	0.013	<u>0.011</u>	Case II 0.009
48	0.33	0.22	0.19	<u>0.15</u>	0.113	Case III 0.15

On each line the periodic coupler whose performance is nearest to that of the synchronously-derived coupler at the end of the line, is underlined. It is seen that roughly twice as many branches are generally required in the periodic coupler to obtain about the same performance. However, the synchronously-derived coupler design has to be adjusted for each bandwidth, as in a quarter-wave transformer or bandpass filter.

**Example VI-2—Comparison of Some 3-db Couplers.** Periodic couplers of 4, 5, 6, and 8 branches<sup>4</sup> were analyzed, as were three synchronous 3-db couplers of four branches each; the synchronous couplers were those used to make up the 0-db couplers for Cases I-III in Example VI-1. Using the same designations for the 3-db couplers, their immittances are given in Table V. (Compare Table II.)

TABLE V  
IMMITTANCES OF THREE SYNCHRONOUS 3-db COUPLERS

IMMITTANCES	CASE I	CASE II	CASE III
$K_0 = K_4$	1.0	.0	1.0
$K_1 = K_3$	1.1563	1.1715	1.1951
$K_2$	1.3852	1.3852	1.3852
$K_0 = K_2$	0.1957	0.2192	0.2500
$K_1$	0.7618	0.7302	0.6955

All of these couplers are derived from quarter-wave transformer prototypes with  $n = 3$ ,  $R = 5.5$ ; their fractional bandwidths,  $w_p$ , are equal to 0.40 for Case I, 0.60 for Case II, and 0.80 for Case III. The performances are summarized in Tables VI and VII. Table VI gives the maximum VSWR over the bandwidths used in Example VI-1. Denote the maximum change in  $P_1$  over any specified bandwidth by  $\Delta P_1$ , and the maximum change in  $P_2$  by  $\Delta P_2$ . To indicate the variation in coupling in a single short table, the quantity  $(|\Delta P_1|_{\max} + |\Delta P_2|_{\max})$  is shown in Table VII, and referred to as the "coupling unbalance."

TABLE VI  
MAXIMUM VSWR OF SEVERAL 3-db COUPLERS OVER STATED BANDWIDTHS

BANDWIDTH (percent)	PERIODIC COUPLERS				FOUR-BRANCH SYNCHRONOUS COUPLERS	
	Four- branch	Five- branch	Six- branch	Eight- branch	Case I	Case II
16	1.02	1.05	1.02	1.01	Case I	1.01
28	1.08	1.10	1.05	1.04	Case II	1.02
48	1.32	1.12	1.15	1.07	Case III	1.07

TABLE VII  
COUPLING UNBALANCE (db) OF SEVERAL 3-db COUPLERS  
OVER STATED BANDWIDTHS

BANDWIDTH (percent)	PERIODIC COUPLERS				FOUR-BRANCH SYNCHRONOUS COUPLERS	
	Four- branch	Five- branch	Six- branch	Eight- branch	Case I	Case II
16	0.20	0.18	0.16	0.14	Case I	0.19
20	0.67	0.51	0.49	0.43	Case II	0.57
40	2.3	1.6	1.5	1.4	Case III	1.9

The four-branch synchronous coupler for each bandwidth has a VSWR as good as, or better than, an eight-branch periodic coupler. The four-branch synchronous coupler is always better in terms of variation in coupling than the four-branch periodic coupler, but not as good as the six-branch periodic coupler.

*Example VI-3—Improved Periodic Couplers.* The periodic coupler designs given by Reed<sup>4</sup> ensure a perfect match at center frequency, and also ensure the specified coupling there. It can be seen from Fig. 16 that if, for instance, the coupling  $P_2$  is to vary as little as possible from some specified value over any non-zero bandwidth, then the coupling  $P_1$  at center frequency should generally be weaker, since  $P_1$  becomes stronger as the frequency deviates from center.

Consider for instance the periodic 0-db coupler of eight branches.<sup>4</sup> By reducing the coupling, which means decreasing the branch immittances, the bandwidth for any specified coupling tolerance can be increased. All of the branch immittances of this coupler were reduced by 4 percent. The VSWR and the insertion loss (coupling  $P_2$ ) of both the original and the modified couplers are plotted in Fig. 25. The improvement in VSWR is only slight, as expected. The bandwidth between the 0.1-db insertion loss points is increased from 42 percent to 49 percent; between the 0.05 db points the increase in bandwidth is from 32 percent to 45 percent. (The curves in Fig. 25 are again symmetrical about the  $\lambda_{gg}/\lambda_g$  axis; hence, only one-half of each curve is shown.)

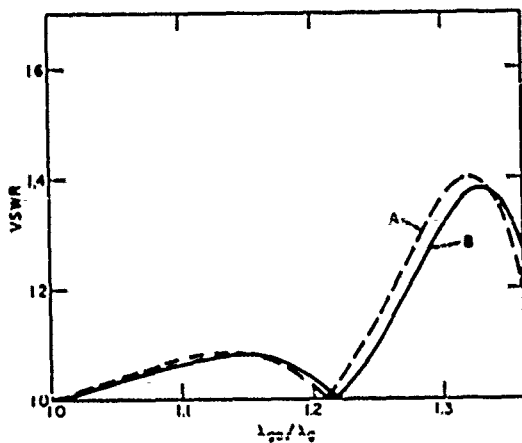
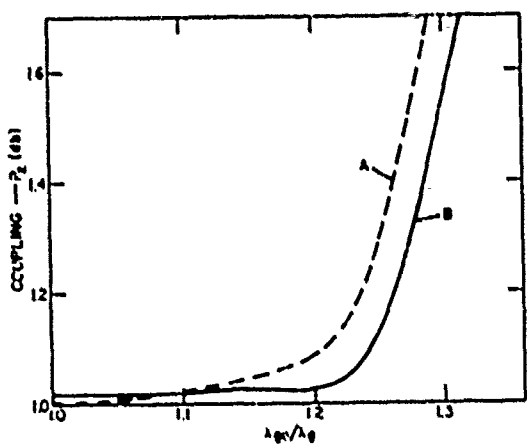


FIG. 25 COMPUTED PERFORMANCE OF TWO EIGHT-BRANCH 0-db PERIODIC COUPLERS (Coupler A after Reed,<sup>4</sup> and Coupler B with branch immittances reduced by 4 percent as in Example VI-3)

## VII EXPERIMENTAL RESULTS

### A. THE 6-db COUPLER

#### 1. CONSTRUCTION

The 6-db coupler of Example V-1 was constructed in S-band. This coupler has five branches. Since waveguide T-junctions are series junctions, the admittances  $K_i$  and  $H_i$  are impedances; however, since waveguide T-junctions are not perfect series junctions, they can be represented by an equivalent circuit<sup>17</sup> such as is shown in Fig. 26. (This is the same circuit as Fig. 6.1-2 on p. 338 of Ref. 17.) At any T-junction of the coupler,  $K_{i-1}$  and  $K_i$  are generally not equal, although they differ only slightly, so that  $K_{av}$  in Fig. 26(a) was set equal to their arithmetic mean  $(K_{i-1} + K_i)/2$ . Similarly the waveguide height substituted into the graphs of Ref. 17 to obtain the T-junction properties was  $b_{av} = (b_{i-1} + b_i)/2$  and the junction was treated as if it were symmetrical [see Fig. 26(b)].

The waveguide heights (their  $b$ -dimensions) were first taken as proportional to the respective  $K$  or  $H$  values [Eq. (14)]; they were fixed by the  $b$ -dimensions of the four ports, which were each equal to  $b_0 = 1.420$  inches. This determined the  $b$ -dimensions in the through-guides without further adjustments, but the  $b$ -dimensions of the

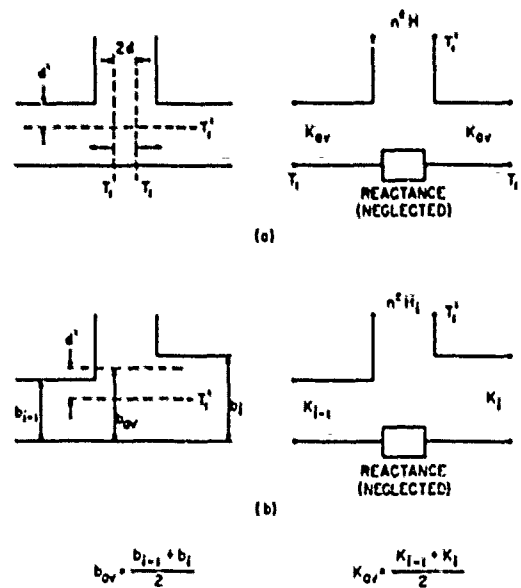


FIG. 26 EQUIVALENT CIRCUITS OF T-JUNCTIONS  
 (a) Symmetrical Junction, after Marcuvitz,<sup>17</sup>  
 (b) Unsymmetrical Junction

branch guides have to be further increased to allow for the transformer factor  $n^2$ . This factor was found from Table 6.1-10 on p. 346 in Ref. 17, and the branch  $b$ -dimensions were increased by a factor  $1/n^2$ . Since this changed the junction dimensions, the quantity  $n^2$  had to be worked out again,<sup>17</sup> and more times if necessary (usually this is not necessary) until each product of  $n^2$  and the branch guide  $b$ -dimension was proportional to the appropriate impedance  $H$ . Finally the reference plane positions,  $d$  and  $d'$ , of each junction were determined<sup>17</sup> (Fig. 26).

Since an  $L$ -band coupler in WR-650 waveguide was later to be scaled from this S-band model, it was designed with output ports in 2.840-inch by 1.420-inch waveguide, to preserve the same two-to-one aspect ratio of WR-650 (6.500 inches by 3.250 inches). Since standard S-band waveguide is WR-284, which is 2.840 inches by 1.340 inches, a two section transformer from 1.420-inch to 1.340-inch waveguide was placed at each port so that all the usual S-band test equipment (slotted line, etc.) could be used. The wide dimension (the so-called  $a$ -dimension) of all waveguides, both inside and outside the coupler, was made 2.840 inches. The  $L$ -band center frequency of 1300 Mc then scaled to 2975 Mc at S-band, and the guide wavelength at center frequency reduced from 12.68 inches to 5.54 inches.

The dimensions of this coupler were calculated, using the impedances of Eq. (14), and the T-junction equivalent circuits in Ref. 17. (The series reactances were included in several of the earlier computations analyzing the coupler performance. Their presence was found to affect the performance only slightly, and has been ignored in all later computations.)

The coupler  $E$ -plane cross-section might be expected to require stepped top and bottom walls (Fig. 1) to obtain the changes in impedance  $K_1$  called for in Eq. (14). However, the reference planes ( $T'_1$  in Fig. 26) move in such a manner that the branches have to be shortened more where the impedances  $K_1$  are larger, with the result that the top and bottom walls (Fig. 1) come out almost straight. In order to obtain straight top and bottom walls as shown in Fig. 1, and yet maintain the correct impedances  $K_1$ , branch lengths some of which differed slightly from the lengths calculated theoretically have to be accepted.

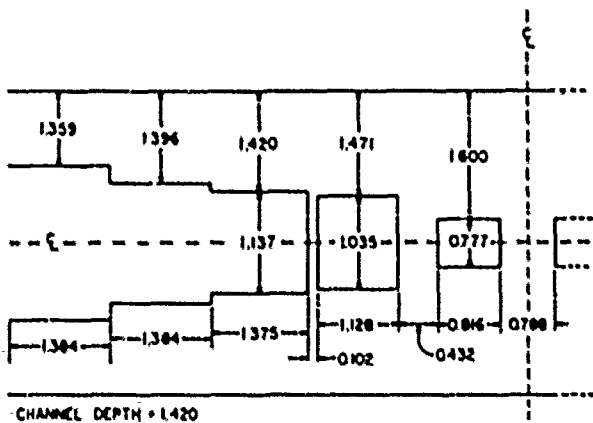


FIG. 27 DIMENSIONS OF FIRST S-BAND 6-db COUPLER -  
BASED ON EXAMPLE V-1

The dimensions so calculated are shown in Fig. 27. The coupler was constructed in two halves as shown in Fig. 28. Three jig-plates of aluminum were used to make a U-shaped channel, in which six aluminum blocks were placed and bolted down to form the waveguide channels. The end blocks contain the transformers from the waveguide height of 1.420 inches to 1.340 inches. The depth of all the channels is half of 2.840 inches, or 1.420 inches. The two pieces shown in Fig. 28 were finally superimposed and bolted together to form the 6-db coupler.

The measured performance of the completed coupler is shown by the light points in Fig. 18, which go with the frequency scale (A) near the bottom of Fig. 18. Plotted on a  $(\lambda_{g0}/\lambda_e)$  scale, the points fit the computed curves very closely; however, the center frequency is 3125 Mc instead of the design value of 2975 Mc. This discrepancy is thought to result from the relatively large *b*-dimensions which, for instance, make the length of an outline edge on the two center squares in Fig. 27 only about one-seventh wavelength. Thus higher-order modes could be set up, giving rise to interaction effects at such close spacings. If this

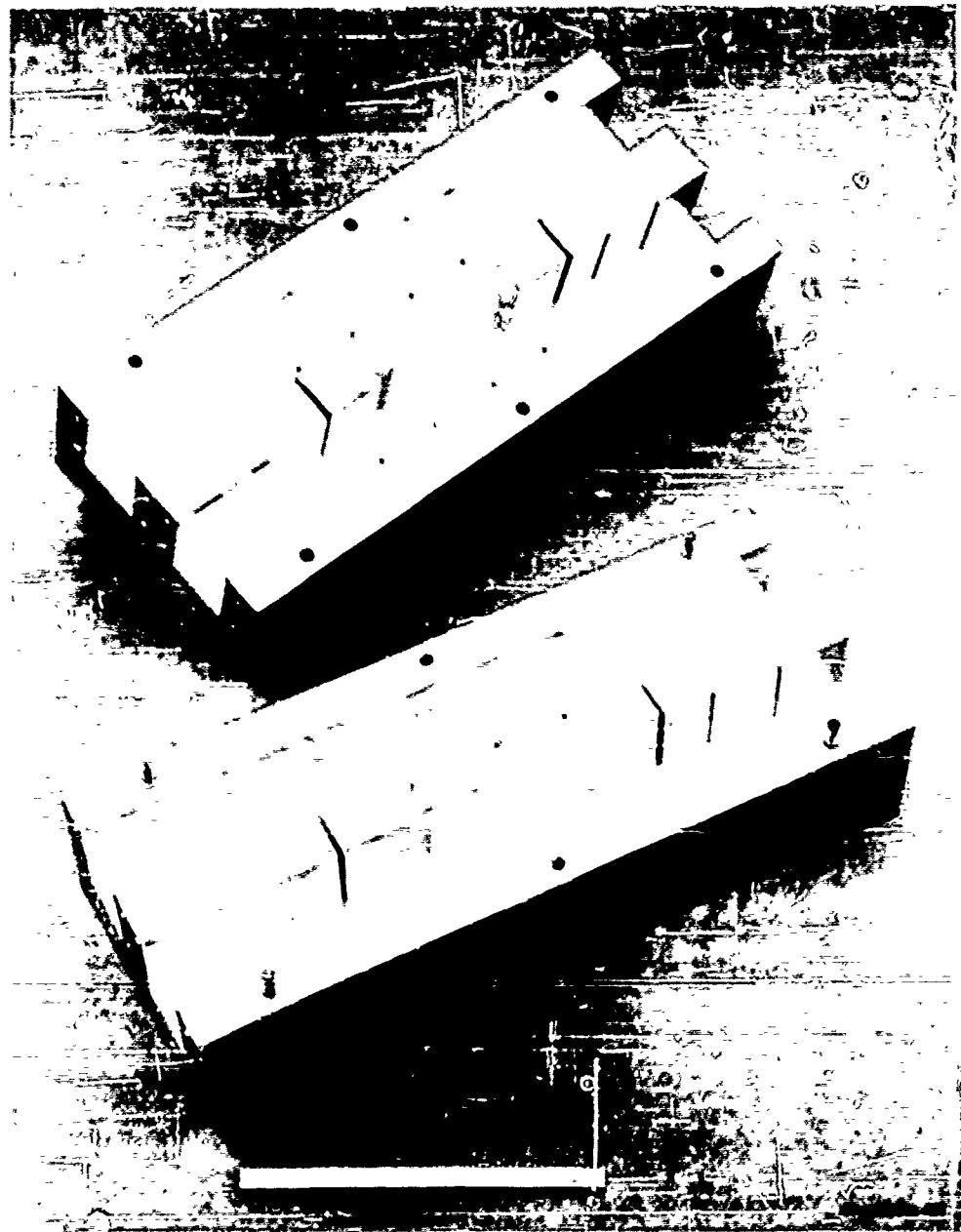


FIG. 28 EXPLODED VIEW OF 6-db EXPERIMENTAL COUPLER

explanation is correct, then lower waveguide heights (smaller  $b$ -dimensions) would result in better design accuracy. However, this was not attempted since the coupler was to be used at high powers where large waveguide heights are an advantage.

All branch lengths and spacings, nominally one-quarter wavelength, were then scaled in the ratio of the guide wavelengths to reduce the center frequency from 3125 to 2975 Mc, and the coupler was tested again. Its center frequency moved down as expected, but the coupling there became stronger, going from 6.1 to 5.8 db. Since the coupling becomes stronger still at off-center frequencies, it was decided to reduce the branch heights to weaken the coupling by 0.5 db at center frequency, changing the 5.8 db to 6.3 db coupling. The new dimensions calculated are shown in Fig. 29. The measured results are shown by the black points

in Fig. 18, which go with the frequency scale (B) at the bottom of Fig. 18. It is seen that this coupler gives the desired center frequency and its performance closely follows the computed curves.

All edges orthogonal to the electric field of the  $TE_{10}$  mode were then rounded off to increase the power handling capacity. The edges of the eight rectangular blocks were rounded to a radius of one-eighth inch; the edges of the four outside blocks, on the faces defining the outside edges of the narrowest branches, were rounded to a radius of one-sixteenth inch. These radii were estimated to reduce the field strength at the edges to less than double the field strength in the waveguides.<sup>18</sup> Any further rounding would have helped very little. The performance of the coupler with rounded edges was measured, and found to reproduce the performance shown in Fig. 18 to within experimental accuracy. The rounding did not introduce any noticeable change in the coupler response.

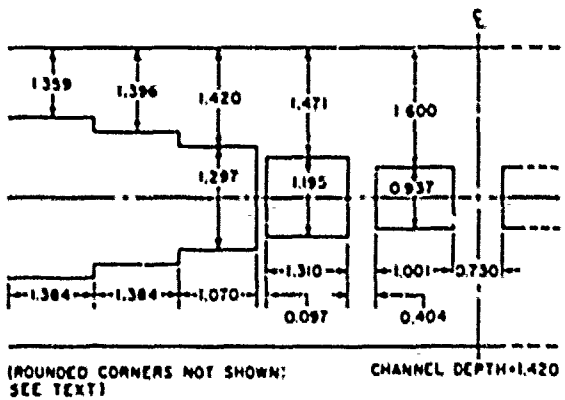


FIG. 29 DIMENSIONS OF S-BAND 6-db COUPLER  
AFTER MODIFICATIONS

## 2. POWER-HANDLING CAPACITY

The power-handling capacity can be estimated as follows. The coupler may be treated as a filter, where the "equivalent power ratio" of Ref. 18 is equal to the internal VSWR for a matched coupler (or almost so for a nearly matched coupler). The highest internal VSWR of the prototype transformer<sup>13</sup> is 1.22 in this case. This VSWR occurs in the second section where the waveguide height is

$$\frac{1.127 \times 1.420}{1.340} = 1.19$$

times the waveguide height of WR-284. If we allow a weakening factor of 2.5 (in power) for the rounded edges (estimated from Ref. 18), this leads us to expect a power-handling capacity of approximately

$$\frac{1.19}{1.22 \times 2.5} = 0.39$$

times the power-handling capacity of WR-284, or roughly 1.0 megawatt in air at atmospheric pressure. (It is assumed that breakdown will not occur first inside the branches.)

The coupler was tested at high power using a 3.6-microsecond pulse at 60 pps, at a frequency of 2857 Mc. With air at atmospheric pressure, no arcing was observed up to at least 1 megawatt peak power. When the power was turned up to 2 megawatts, there was some arcing, but this appeared to be caused by a waveguide bend.

## B. THE 0-dB COUPLER

### 1. CONSTRUCTION

The 0-dB coupler is constructed following the procedure of Example V-2. It is based on the 6-db experimental coupler just described, but scaled from S-band to L-band, with the ratio of the two guide wavelengths at center frequency as the scaling factor. The ratio of the guide wavelengths was made equal to the ratio of the a-dimensions of WR-650 and WR-284.

The coupler was constructed of aluminum jig-plate in the fashion described for the 6-db coupler. The over-all length was close to four feet,

so that it was made in two flanged sections, which bolted together. The dimensions of one-half the coupler are given in Fig. 30. A photograph of the entire coupler is shown in Fig. 31.

The measured performance of this coupler is shown in Figs. 19 and 20, and it is found to agree very closely with the computed curves.

## 2. POWER-HANDLING CAPACITY

The edges perpendicular to the electric field were rounded to a  $\frac{1}{8}$ -inch radius, except for an  $\frac{1}{16}$ -inch radius on the end blocks, to increase the power-handling capacity. (Compare the 6-db coupler.) This was found to have no measurable effect on the performance. Using the estimate for the 6-db coupler, the power-handling capacity should be about  $(6.5/2.84)^2 \times 1.0$  megawatt, or 5.2 megawatts in air at atmospheric pressure.

High-power tests were made using the Eimac X832 experimental Klystron amplifier, which operates at *L*-band and supplies 2-microsecond pulses at 60 pps. A cobalt-60 radioactive source was placed under the coupler\* to insure that the air was ionized at points most susceptible to breakdown. The branch-guide coupler was filled with air at atmospheric pressure. It did not break down at the peak power available, which was 5.1 megawatts. The VSWR of the wave-load at the output of the coupler was 1.3, but as no phase shifter was available, it is not known how much it helped or hurt the power handling capacity. However, it is probably safe to say that this coupler would handle at least 5 megawatts of peak power in air at atmospheric pressure with a matched termination.

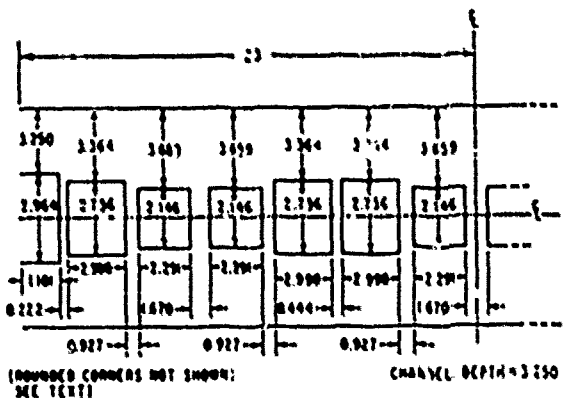


FIG. 30 DIMENSIONS OF 0-db COUPLER  
(Only half the coupler is shown)

\* The circuit tested was the two halves of the 0-db coupler, arranged as two 3-db couplers as explained in connection with Fig. 36, rather than the coupler described above. One 3-db coupler had the slots shown in the photograph of Fig. 36, but the other 3-db coupler was without any slots, as described above. Since each 3-db coupler (half a 0-db coupler) had a good VSWR by itself, this test is essentially the same as testing a complete 0-db coupler with or without slots.

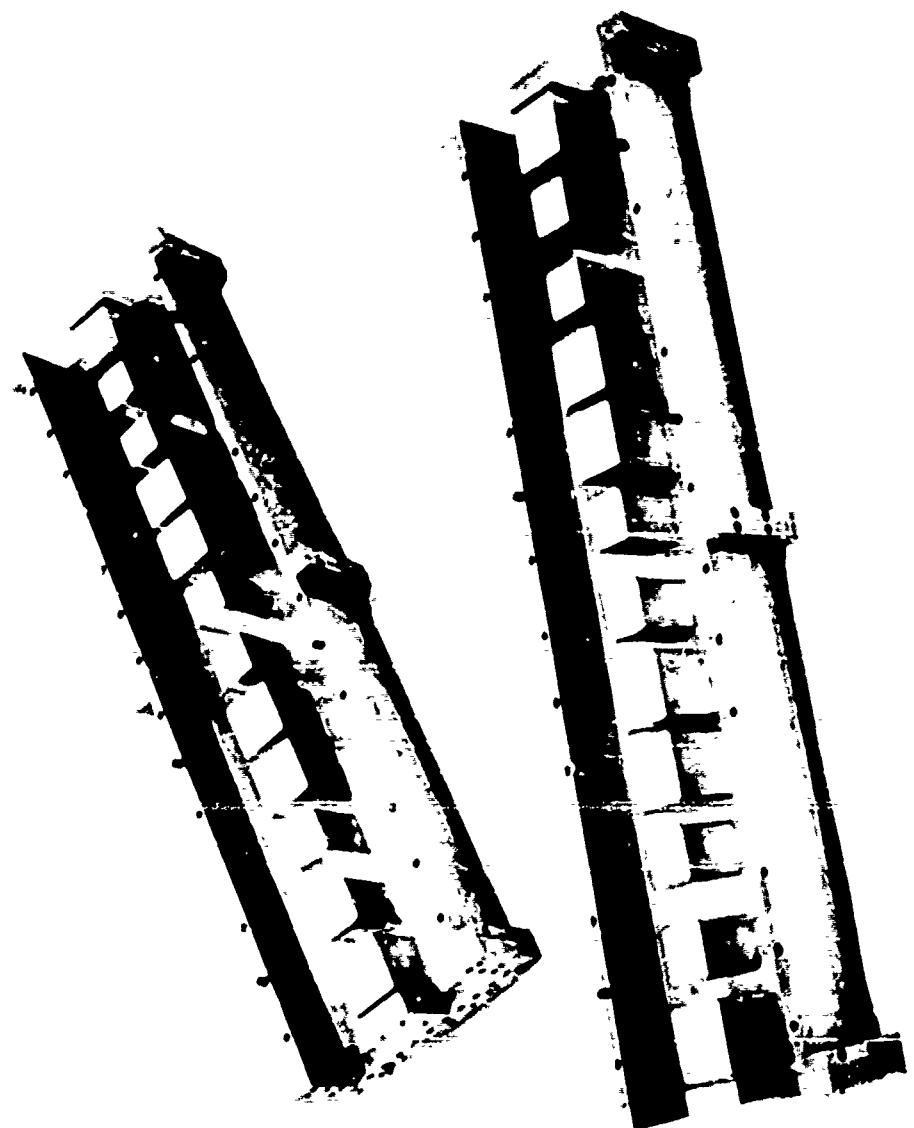


FIG. 31 EXPLODED VIEW OF FIRST O-Jb EXPERIMENTAL COUPLING

### 3. ABSORPTION OF HIGHER FREQUENCIES

The purpose of the 0-db coupler was to act as an absorption filter for harmonic and other spurious frequencies in the power output of high-power microwave tubes.\* It is used in conjunction with a rejection filter, such as a waffle-iron filter. The 0-db coupler is placed between the transmitter and the rejection filter to protect the tube from the reflected spurious frequencies. It is not necessarily required to provide high attenuation at the spurious frequencies (this is accomplished by the rejection filter), but to provide enough attenuation that a satisfactory match can be presented to the transmitter, even when an effective short-circuit is placed at the output of the 0-db coupler at the spurious frequencies.

Figure 32 indicates the reasoning behind this arrangement. The coupler is designed as a cross-over (0-db) coupler at the fundamental-frequency output. At higher frequencies, the coupling into the branches decreases ( $n^2$  in Fig. 6.1-10 on p. 346 of Ref. 17 decreases). The higher frequencies will therefore tend to be "beamed" through to the load instead of crossing over, thereby becoming separated from the fundamental frequency without being reflected. This is, of course, only a qualitative argument, and applies best to the  $TE_{10}$  and the lower-order modes. For instance, all  $TE_{10}$  modes, as they approach cutoff, will pass through a frequency at which the guide wavelength is 12.68 inches, the  $\lambda_{g0}$  of the fundamental band-center in the  $TE_{10}$  mode. This gives rise to frequency bands, which in certain modes will suffer no attenuation in the coupler. This was confirmed experimentally for the  $TE_{30}$  mode at 2600 Mc.

It was also found in the  $TE_{10}$  mode around 2600 Mc that the coupling was as strong as 1.5 db, resulting in a high VSWR when the rejection filter or a short circuit was placed at the output. The explanation for

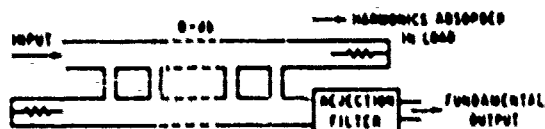


FIG. 32 ARRANGEMENT OF 0-DB COUPLER AND SPURIOUS-FREQUENCY REJECTION FILTER

\* This application seems to have been first suggested by Vernon Price, and was suggested independently by the author at a later date.

this is probably that at this frequency the guide wavelength is such that the branch lengths and spacings are approximately three-quarters guide wavelength long. If the couplings and reference planes had remained constant, 0-db coupling would have been obtained at this frequency.

Since this strong coupling occurs at the second harmonic of the center frequency, which might be expected to be strongly present in the output from a high-power transmitter, it was decided to reduce the second-harmonic coupling by placing chokes in all the branches. This would prevent the second harmonic from crossing over. (A more general solution would be to build appropriate filters in the branches.) These second-harmonic chokes were placed in the mid-plane of the branches, and the branch impedances were reduced to compensate for their reactances at 1300 Mc. The calculation is given in Appendix III. The dimensions are given in Fig. 33, and a photograph of the coupler is given in Fig. 34. The measured pass-band insertion loss is plotted in Fig. 35; the insertion loss is better than 0.1 db from about 1150 to 1350 Mc. The pass band has become narrower as a result of the chokes, and the center frequency has moved down. However, since the performance over the band 1300  $\pm$  50 Mc was adequate, no experimental adjustment was made to raise the center frequency. The edges of the T-junctions at the open ends of the chokes were then rounded to a radius of  $\frac{1}{8}$  inch to improve the power-handling capacity.

This coupler presented a low VSWR to the second harmonic in the  $TE_{10}$  mode with or without a short-circuit at the output. Further improvement in the  $TE_{10}$  mode was obtained with the circuit of Fig. 36. This photograph shows the two halves of the 0-db coupler used as two

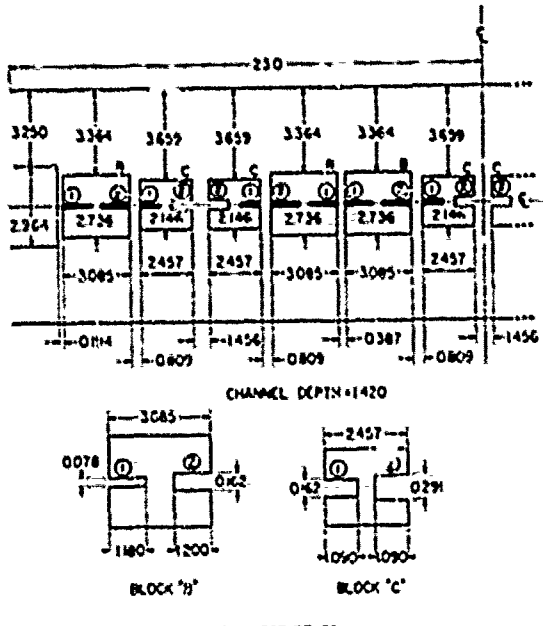


**FIG. 33 DIMENSIONS OF 0-dB COUPLER WITH SECOND-HARMONIC CHOKES  
(Only half the coupler is shown)**

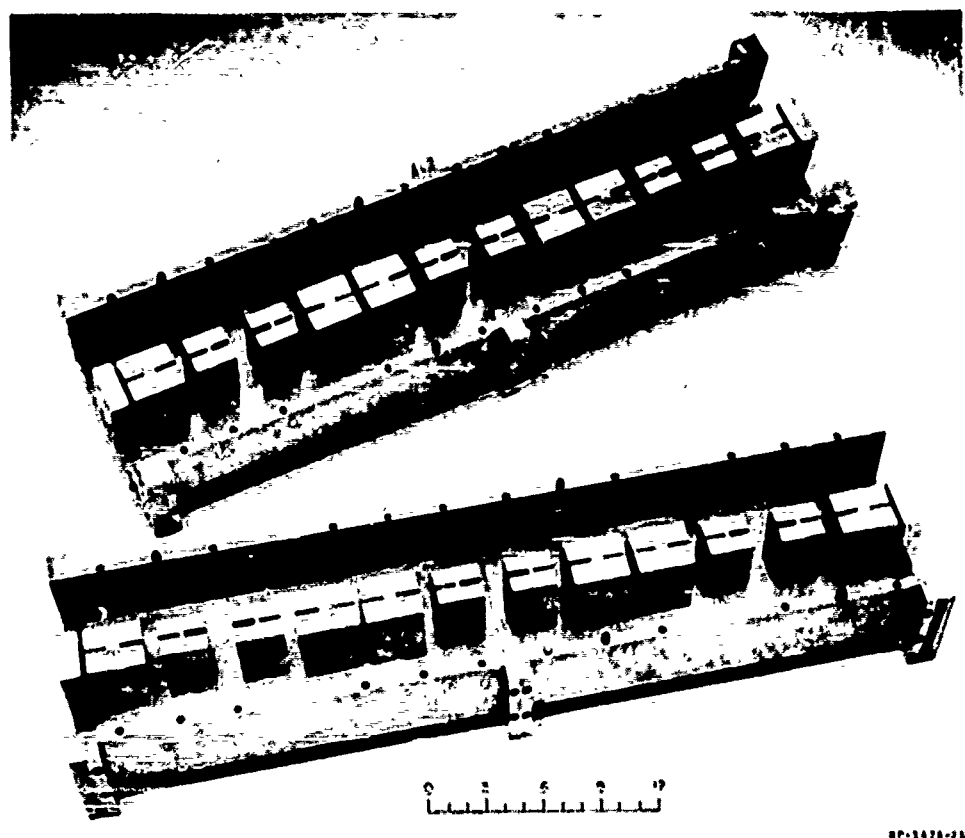


FIG. 34 EXPLODED VIEW OF 0-dB COUPLER WITH SECOND-HARMONIC CHOKES

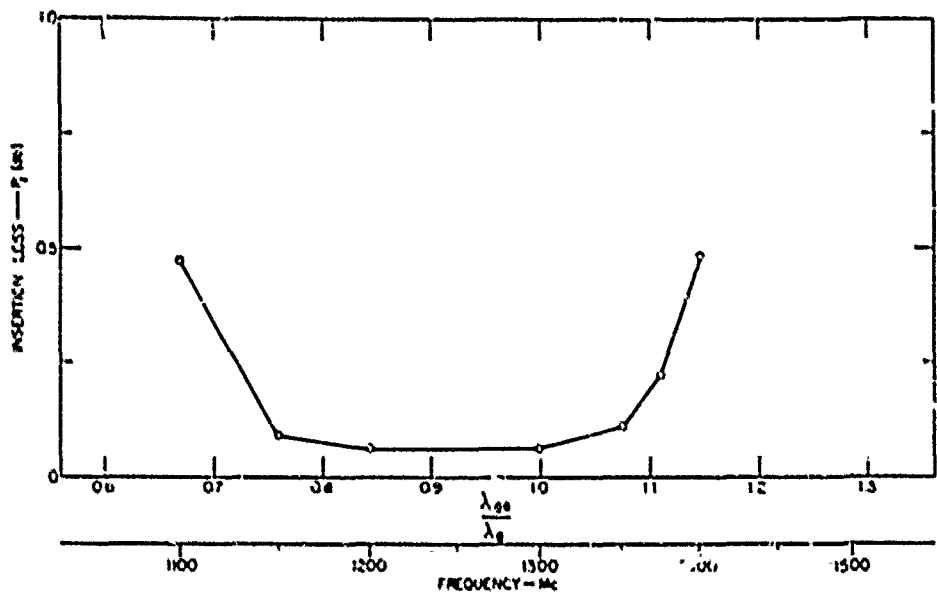


FIG. 35 MEASURED INSERTION LOSS OF 0-dB COUPLER WITH SECOND-HARMONIC CHOKES

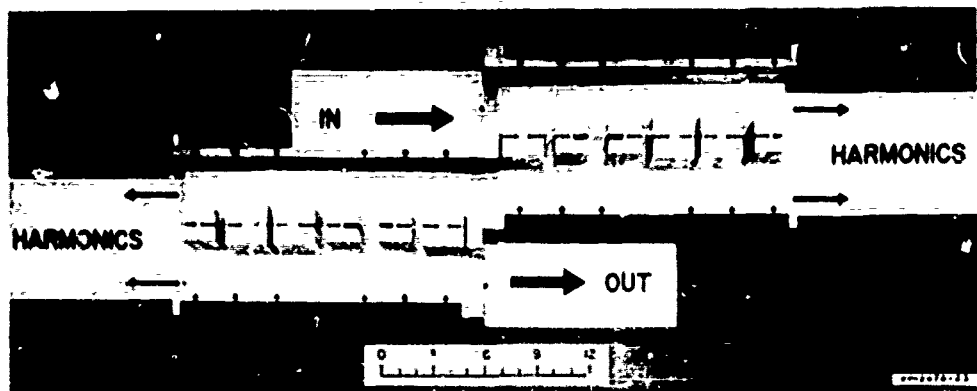


FIG. 36 ARRANGEMENT OF TWO 3-dB COUPLERS TO SUPPRESS SPURIOUS FREQUENCIES

3-db couplers. (Each 3-db coupler is one-and-one-half 6-db couplers, and had a VSWR below 1.10.) Each 3-db coupler is connected to two waveguides that taper from 6.500 inches by 3.250 inches waveguide to 3.750 inches by 3.250 inches waveguide (Fig. 37). This guide is cut-off in the fundamental pass band, but transmits all harmonic frequencies in the  $TE_{10}$  and most other modes. Such an arrangement has the advantage of simplicity, but it also has the disadvantage of reflecting some important frequencies in certain likely modes (as for instance the second harmonic in the  $TE_{10}$  mode). It should be possible to devise something better for this purpose than a tapered waveguide, which, however, was retained because of its simplicity.

The photograph in Fig. 36 shows both 3-db couplers as containing slotted blocks. (The "slots" are the second-harmonic chokes.) It was felt that a better arrangement would be to have the chokes only in the first 3-db coupler (nearest the input), and to have only plain blocks without chokes (compare Fig. 31) in the second 3-db coupler. All of the subsequent measurements were made with this modification applied to the arrangement shown in Fig. 36.

At low power, long tapered waveguide sections were used to set up the  $TE_{10}$  mode at frequencies ranging from 2.2 Gc (below the second harmonic) to 15.4 Gc (above the eleventh harmonic). A bank of motor-driven swept signal generators was used to generate the input, and the output was recorded on a pen-recorder synchronized with the motor driving the signal-generator tuning-knob. Matched loads were placed at the output of the four cutoff waveguides. The reflection coefficient thus obtained at the input to the long taper was measured by recording (1) the incident power and (2) the reflected power with the arrangement of Fig. 36 followed by a waffle-iron rejection filter (which acts as a short circuit from 2 Gc up to at least 14 Gc) as shown in Fig. 37. These two recorded curves are shown in Fig. 38. The reflection coefficient in decibels, at any frequency, is the distance between the two curves. The harmonic bands of 1250-1350 Mc are marked in Fig. 38. It is seen that the reflected power at the input is at least 10 db below the input power, in all the harmonic bands from the second to the eleventh, which corresponds to a VSWR (at the input to the taper launching the  $TE_{10}$  mode) of better than 2:1.

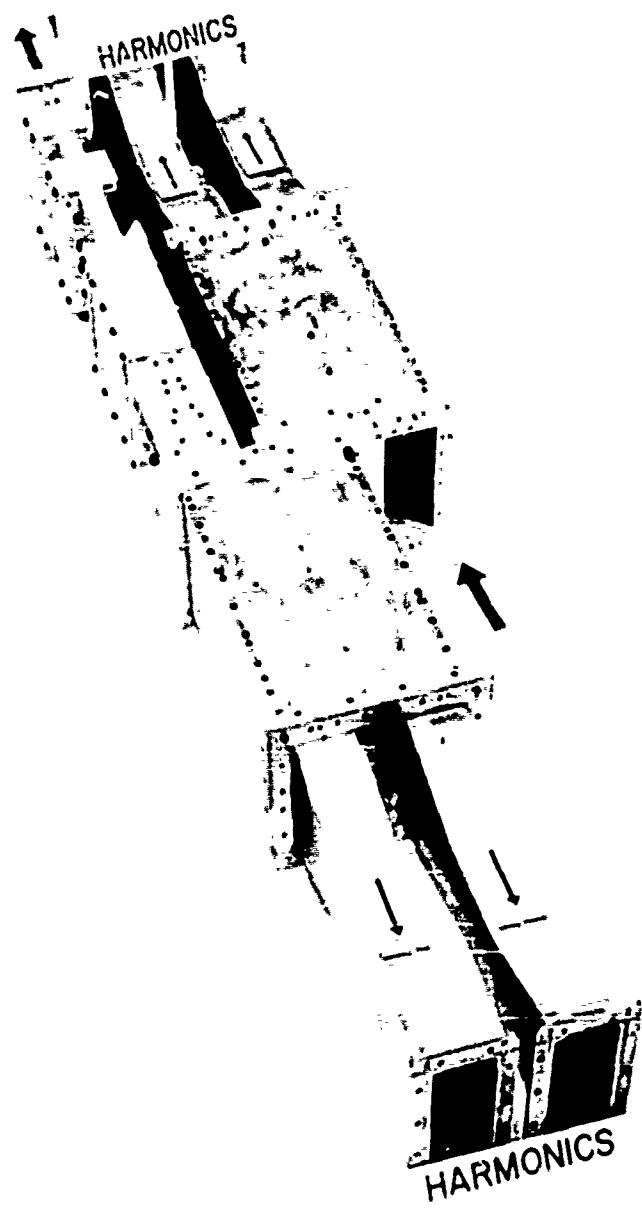


FIG. 37 VIEW OF COMPLETE FILTER FOR SUPPRESSION OF SPURIOUS FREQUENCIES,  
SHOWING BRANCH-GUIDE COUPLERS (Middle), WAVEGUIDE TAPERS (Foreground  
and Upper Right), AND WAFFLE-IRON FILTER (Upper Left)

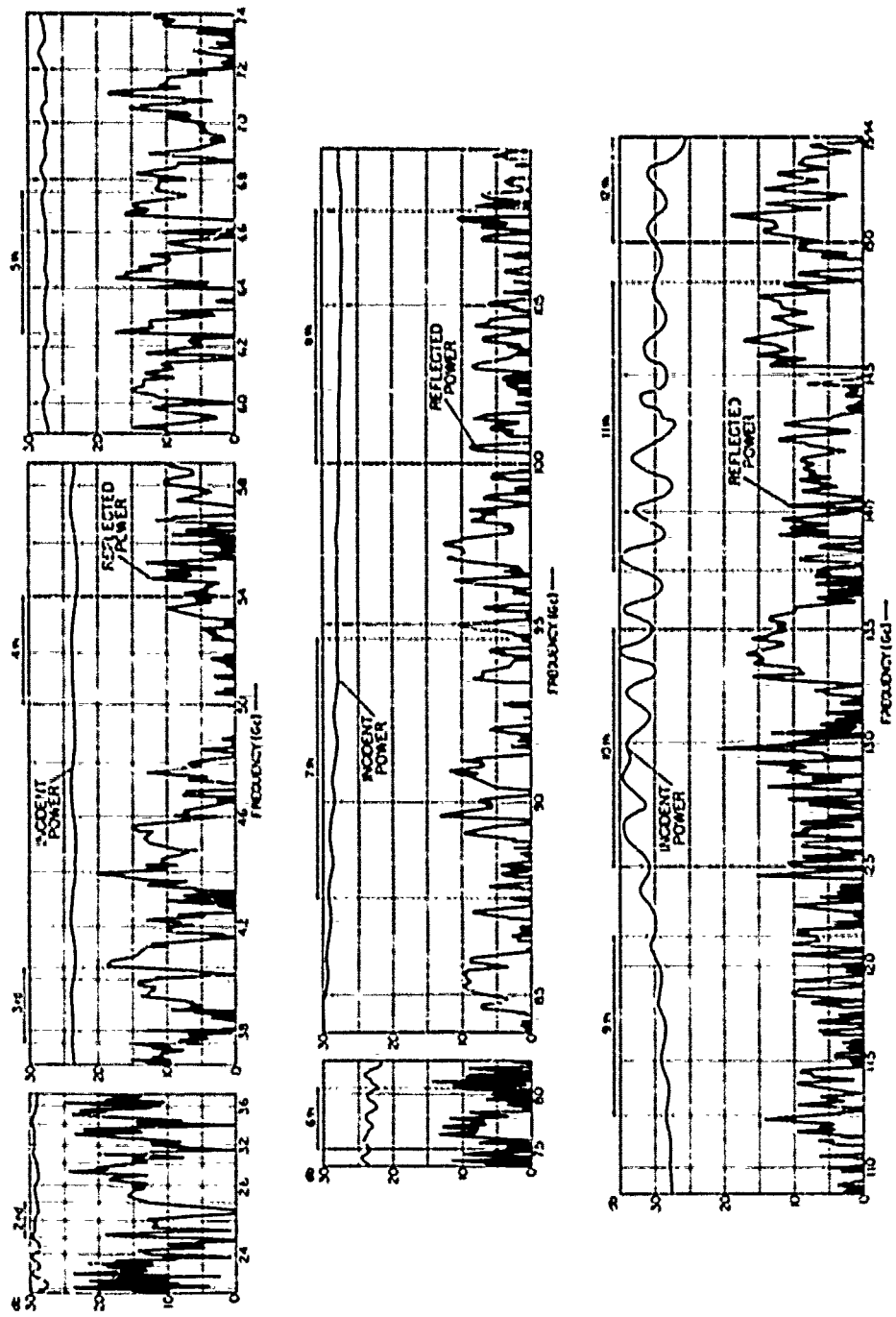


FIG. 38 INCIDENT AND REFLECTED POWERS IN THE  $TE_{11}$  MODE FROM THE SECOND TO THE ELEVENTH HARMONIC WITH THE FILTER OF FIG. 37

At high power, the coupler configuration of Fig. 35 (again with no chokes in the second coupler) was tested up to 5.1 megawatts peak power, as already described. Since the predicted power handling capacity is 5.2 megawatts for the coupler without chokes, it may be concluded that the addition of chokes in the branches does not appreciably affect its power-handling capacity.

## VIII CONCLUSION

A design method for branch-guide couplers has been developed which gives close to optimum performance over a given pass-band. The method was tested by analyzing the performance of several numerical designs, then constructing two couplers in waveguide and comparing the actual with the computed characteristics. The agreement was close. The design procedure is facilitated by a new chart constructed for this purpose; alternatively, most practical cases can be worked out from the tables in Appendix I by interpolation.

The 0-db branch-guide coupler has been used as a harmonic pad (that is, a harmonic absorber in front of a harmonic rejection filter). Measurements to date have been confined to the  $TE_{11}$  mode, for which the padding achieved should be adequate for most practical purposes. A VSWR of better than 2:1 has been obtained at all harmonic frequencies up to the eleventh harmonic. The absorption of spurious frequencies improves as the frequency increases.

The L-band 0-db coupler has passed over 5 megawatts of peak power in air at atmospheric pressure without any sign of arcing.

## BIBLIOGRAPHY

1. H. A. Lippmann, "Theory of Directional Couplers," MIT Rad. Lab. Report 850, Massachusetts Institute of Technology, Cambridge, Massachusetts (December 28, 1945).
2. J. Reed and G. Sheeler, "A Method of Analysis of Symmetrical Four-Port Networks," *IRE Trans. on Microwave Theory and Techniques*, Vol. MTT-4, pp. 246-252 (October 1956).
3. Leo Young, "Branch Guide Directional Couplers," *Proc. Nat. Electronics Conf.*, Vol. 12, pp. 723-732, 1956. (There is a misprint for the S-branch coupler in Table I. The expression for  $Y$  contains a term  $PKH$ , which should have been  $PKH^2$ .)
4. J. Reed, "The Multiple Branch Waveguide Coupler," *IRE Trans. on Microwave Theory and Techniques*, Vol. MTT-8, pp. 398-403 (October 1958).
5. P. D. Lower and J. W. Crompton, "A New Form of Hybrid Junction for Microwave Frequencies," *Proc. IEE (London)*, Part B, Vol. 104, pp. 261-264 (May 1957).
6. J. W. Crompton, "A Contribution to the Design of Multi-Element-Directional Couplers," *Proc. IEE (London)*, Part C, Vol. 104, pp. 398-402 (September 1957).
7. S. H. Cohn, "Direct-Coupled-Resonator Filters," *Proc. IRE*, Vol. 45, pp. 187-196 (February 1957).
8. G. L. Matthaei, "Design of Wide-Band (and Narrow-Band) Band-Pass Microwave Filters on the Insertion Loss Basis," *IRE Trans. on Microwave Theory and Techniques*, Vol. MTT-8, pp. 580-593 (November 1960).
9. Leo Young, "The Quarter-Wave-Transformer Prototype Circuit," *IRE Trans. on Microwave Theory and Techniques*, Vol. MTT-8, pp. 483-489 (September 1960).
10. H. J. Hilett, "General Synthesis of Quarter-Wave Impedance Transformers," *IRE Trans. on Microwave Theory and Techniques*, Vol. MTT-8, pp. 36-43 (January 1957).
11. Leo Young, "Synthesis of Multiple Antireflection Films Over a Prescribed Frequency Band," *Jour. Opt. Soc. Am.*, Vol. 51, pp. 967-974 (September 1961).
12. Leo Young, "Tables for Cascaded Homogeneous Quarter-Wave Transformers," *IRE Trans. on Microwave Theory and Techniques*, Vol. MTT-7, pp. 233-237 (April 1959) and Vol. MTT-8, pp. 243-244 (March 1960).
13. L. Young and G. L. Matthaei, "Microwave Filters and Coupling Structures," Fourth Quarterly Progress Report, SRI Project 3527, Contract DA 36-039 SC-87398, Stanford Research Institute, Menlo Park, California (February 1962).
14. H. W. Bode, *Network Analysis and Feedback Amplifier Design* (D. Van Nostrand Co., New York, New York, September 1945).
15. P. H. Smith, "Transmission Line Calculator," *Electronics*, Vol. 12, pp. 29-31 (January 1939); and "An Improved Transmission Line Calculator," *Electronics*, Vol. 17, pp. 130-133 and 318-325 (January 1944).
16. P. S. Carter, "Charts for Transmission-Line Measurements and Computations," *ACA Review*, Vol. 3, pp. 355-368 (January 1939).
17. N. Marcuvitz, *Waveguide Handbook*, pp. 336-350, MIT Rad. Lab. Series, Vol. 10 (McGraw-Hill Book Co., Inc., New York New York, 1951).
18. S. H. Cohn, "Bounded Corners in Microwave High-Power Filters and Other Components," *IRE on Microwave Theory and Techniques*, Vol. MTT-9, pp. 389-397 (September 1961).
19. Leo Young, "Peak-Internal-Fields in Direct-Coupled-Cavity Filters," *IRE Trans. on Microwave Theory and Techniques*, Vol. MTT-8, pp. 612-616 (November 1960).

## APPENDIX I

## TABLES OF BRANCH-GUIDE COUPLER IMPEDANCES

The notation for the impedances  $H_i$  and  $K_i$  is shown in Fig. 2. For a coupler with series T-junctions,  $H_i$  and  $K_i$  are both characteristic impedances (e.g. for E-plane junctions in waveguide); for a coupler with shunt T-junctions,  $H_i$  and  $K_i$  are both characteristic admittances (e.g. for coaxial or strip transmission lines).

TABLE I-1  
BRANCH-GUIDE COUPLER IMPEDANCES  
FOR  $\kappa = 1$  SECTION (TWO BRANCHES)

$\kappa = 1$		
$R$	$K_1$	$K_0$
1.00	1.006	0.1119
1.50	1.021	0.2040
2.00	1.061	0.3535
2.50	1.108	0.4732
3.00	1.155	0.5775
4.00	1.250	0.7500
5.00	1.341	0.894
6.00	1.429	1.021
8.00	1.592	1.238
10.00	1.739	1.423

TABLE I-2  
IMMITTANCES OF MAXIMALLY FLAT BRANCH-GUIDE COUPLERS FOR  $n = 2$  TO 8 SECTIONS  
(THREE, TO NINE, BRANCHES)

$n$	$R$	$R_1$	$R_2$	$R_3$	$R_4$	$R_5$	$R_6$	$R_7$	$R_8$	$R_9$
$n = 2$										
1.50	1.0153					0.1010	0.2042			
2.00	1.0419					0.1715	0.3619			
2.50	1.0783					0.2251	0.4943			
3.00	1.1128					0.2679	0.6188			
4.00	1.1745					0.3333	0.8333			
5.00	1.2399					0.3819	1.0249			
6.00	1.2965					0.4202	1.2004			
8.00	1.3976					0.4775	1.5196			
10.00	1.4861					0.5194	1.8070			
$n = 3$										
1.50	1.0069	1.0206				0.0501	0.1539			
2.00	1.0258	1.0606				0.0840	0.2694			
2.50	1.0446	1.1067				0.1086	0.3654			
3.00	1.0634	1.1546				0.1274	0.4476			
4.00	1.0948	1.2459				0.1542	0.5957			
5.00	1.1307	1.3416				0.1732	0.7220			
6.00	1.1594	1.4288				0.1853	0.8551			
8.00	1.2047	1.5909				0.2029	1.0344			
10.00	1.2501	1.7392				0.2138	1.2091			
$n = 4$										
1.50	1.0047	1.0176				0.0249	0.1017	0.1548		
2.00	1.0137	1.0517				0.0415	0.1750	0.2738		
2.50	1.0235	1.0907				0.0533	0.2331	0.3758		
3.00	1.0333	1.1307				0.0620	0.2814	0.4676		
4.00	1.0514	1.2093				0.0740	0.3596	0.6326		
5.00	1.0675	1.2835				0.0817	0.4220	0.7811		
6.00	1.0816	1.3530				0.0870	0.4743	0.9185		
8.00	1.1057	1.4795				0.0935	0.5589	1.1698		
10.00	1.1256	1.5924				0.0971	0.6265	1.3906		
$n = 5$										
1.50	1.0024	1.0124	1.0206			0.0124	0.0630	0.1285		
2.00	1.0070	1.0363	1.0625			0.0206	0.1069	0.2259		
2.50	1.0121	1.0630	1.1067			0.0264	0.1800	0.3079		
3.00	1.0170	1.0902	1.1546			0.0306	0.1662	0.3804		
4.00	1.0262	1.1421	1.2499			0.0363	0.2058	0.5078		
5.00	1.0342	1.1899	1.3416			0.0398	0.2348	0.5196		
6.00	1.0413	1.2335	1.4288			0.0422	0.2573	0.7210		
8.00	1.0532	1.3106	1.5909			0.0450	0.2904	0.9019		
10.00	1.0630	1.3769	1.7392			0.0464	0.3140	1.0625		
$n = 6$										
1.50	1.0012	1.0079	1.0185			0.0062	0.0376	0.0957	0.1290	
2.00	1.0035	1.0230	1.0544			0.0103	0.0631	0.1658	0.2284	
2.50	1.0061	1.0397	1.0956			0.0131	0.0817	0.2225	0.3138	
3.00	1.0086	1.0564	1.1380			0.0152	0.0959	0.2707	0.3908	
4.00	1.0132	1.0878	1.2216			0.0180	0.1162	0.3509	0.5295	
5.00	1.0172	1.1161	1.3010			0.0197	0.1301	0.4170	0.6549	
6.00	1.0208	1.1414	1.3758			0.0208	0.1402	0.4738	0.7712	
8.00	1.0268	1.1852	1.5128			0.0221	0.1539	0.5689	0.9846	
10.00	1.0317	1.2220	1.6361			0.0228	0.1626	0.6477	1.1796	
$n = 7$										
1.50	1.0006	1.0047	1.0143	1.0206		0.0031	0.0218	0.0665	0.1126	
2.00	1.0018	1.0137	1.0419	1.0606		0.0051	0.0364	0.1135	0.1983	
2.50	1.0030	1.0236	1.0731	1.1067		0.0065	0.0468	0.1499	0.2109	
3.00	1.0043	1.0334	1.1048	1.1546		0.0076	0.0546	0.1795	0.3355	
4.00	1.0066	1.0516	1.1662	1.2499		0.0089	0.0653	0.2258	0.4497	
5.00	1.0086	1.0678	1.2231	1.3416		0.0098	0.0724	0.2612	0.5509	
6.00	1.0104	1.0822	1.2759	1.4288		0.0103	0.0772	0.2898	0.6431	
8.00	1.0134	1.1067	1.3699	1.5909		0.0110	0.0834	0.3332	0.8090	
10.00	1.0159	1.1270	1.4520	1.7392		0.0113	0.0869	0.3672	0.9574	
$n = 8$										
1.50	1.0003	1.0027	1.0101	1.0190		0.0015	0.0124	0.0440	0.0895	0.1129
2.00	1.0009	1.0079	1.0293	1.0559		0.0025	0.0207	0.0743	0.1558	0.2000
2.50	1.0015	1.0135	1.0508	1.0982		0.0032	0.0265	0.0969	0.2100	0.2748
3.00	1.0021	1.0191	1.0724	1.1419		0.0037	0.0308	0.1146	0.2567	0.3425
4.00	1.0033	1.0295	1.1134	1.2282		0.0044	0.0366	0.1408	0.3357	0.4644
5.00	1.0043	1.0386	1.1508	1.3104		0.0049	0.0402	0.1595	0.4021	0.5749
6.00	1.0052	1.0467	1.1846	1.3881		0.0051	0.0427	0.1737	0.4601	0.6775
8.00	1.0067	1.0603	1.2436	1.5308		0.0055	0.0457	0.1939	0.5591	0.8661
10.00	1.0080	1.0715	1.2940	1.6598		0.0056	0.0474	0.2078	0.6426	1.0388

TABLE I-3  
IMMITTANCES OF MIANCH-GUIDE COUPLERS FOR  $n = 2$ , 3 AND 4 SECTIONS  
(THREE, FOUR, AND FIVE BRANCHES) WHEN  $\nu_0 = 0.20$

$n$	$K_1$	$K_2$	$K_3$	$K_4$	$K_5$
$n = 2$					
1.50	1.0155		0.1022	0.2046	
2.00	1.0453		0.1738	0.3594	
2.50	1.0790		0.2282	0.4922	
3.00	1.1135		0.2717	0.6111	
4.00	1.1803		0.3385	0.8229	
5.00	1.2425		0.3883	1.0121	
6.00	1.3000		0.4276	1.1859	
8.00	1.4029		0.4870	1.5007	
10.00	1.4929		0.5307	1.7845	
$n = 3$					
1.50	1.0090	1.0206	0.0511	0.1530	
2.00	1.0262	1.0606	0.0856	0.2678	
2.50	1.0454	1.1067	0.1108	0.3634	
3.00	1.0645	1.1516	0.1300	0.4473	
4.00	1.1006	1.2499	0.1574	0.5925	
5.00	1.1331	1.3416	0.1761	0.7182	
6.00	1.1624	1.4288	0.1897	0.8309	
8.00	1.2129	1.5909	0.2078	1.0295	
10.00	1.2554	1.7392	0.2193	1.2036	
$n = 4$					
1.50	1.0048	1.0177	0.0256	0.1017	0.1535
2.00	1.0140	1.0519	0.0426	0.1751	0.2715
2.50	1.0211	1.0909	0.0517	0.2332	0.3727
3.00	1.0341	1.1311	0.0636	0.2817	0.4638
4.00	1.0527	1.2099	0.0760	0.3602	0.5274
5.00	1.0692	1.2844	0.0839	0.4230	0.7747
6.00	1.0837	1.3513	0.0894	0.4756	0.9110
8.00	1.1085	1.4811	0.0962	0.5610	1.1603
10.00	1.1290	1.5919	0.1000	0.6293	1.3872

TABLE I-4  
IMMITTANCES OF MACHOI-GUING COUPLERS FOR  $n = 2, 3$  AND 4 SECTIONS  
(THREE, FOUR, AND FIVE MACHINES) WHEN  $\mu_s = 0.40$

$n$	$\kappa_1$	$\kappa_2$	$\kappa_1$	$\kappa_2$	$\kappa_3$
$n = 2$					
1.50	1.0159		0.1061	0.1958	
2.00	1.0464		0.1907	0.3455	
2.50	1.0811		0.2376	0.4733	
3.00	1.1164		0.2835	0.5876	
4.00	1.1857		0.4543	0.7913	
5.00	1.2503		0.4074	0.9731	
6.00	1.3102		0.4506	1.1400	
8.00	1.4181		0.5162	1.4424	
10.00	1.5132		0.5635	1.7146	
$n = 3$					
1.50	1.0095	1.0206	0.0510	0.1500	
2.00	1.0275	1.0604	0.0907	0.2627	
2.50	1.0477	1.1067	0.1176	0.3567	
3.00	1.0679	1.1546	0.1381	0.4391	
4.00	1.1061	1.2499	0.1678	0.5821	
5.00	1.1407	1.3416	0.1882	0.7052	
6.00	1.1719	1.4288	0.2031	0.8174	
8.00	1.2260	1.5909	0.2235	1.0139	
10.00	1.2718	1.7392	0.2367	1.1862	
$n = 4$					
1.50	1.0052	1.0178	0.0276	0.1016	0.1497
2.00	1.0150	1.0523	0.0459	0.1751	0.2647
2.50	1.0259	1.0917	0.0590	0.2335	0.3634
3.00	1.0367	1.1323	0.0688	0.2823	0.4522
4.00	1.0567	1.2119	0.0823	0.3617	0.6117
5.00	1.0745	1.2873	0.0911	0.4255	0.7554
6.00	1.0904	1.3580	0.0972	0.4791	0.8884
8.00	1.1173	1.4869	0.1048	0.5667	1.1313
10.00	1.1397	1.6023	0.1093	0.6373	1.3528

TABLE I-C  
TRANSMITTANCES OF BRANCH-GUIDE COUPLINGS FROM  $n = 2, 3$  AND  $4$  SECTIONS  
(THREE, FOUR, AND FIVE MACHINES) WHEN  $\nu = 0.60$

$A$	$\#_1$	$\#_2$	$\#_1$	$\#_2$	$\#_3$
$n = 2$					
1.50	1.0165		0.1126	0.1824	
2.00	1.0483		0.1925	0.3220	
2.50	1.0846		0.2539	0.4408	
3.00	1.1218		0.3037	0.5471	
4.00	1.1945		0.3818	0.7363	
5.00	1.2630		0.4118	0.9051	
6.00	1.3269		0.4906	1.0598	
8.00	1.4130		0.5671	1.3398	
10.00	1.5164		0.6271	1.5917	
$n = 3$					
1.50	1.0103	1.0206	0.0594	0.1446	
2.00	1.0299	1.0606	0.1009	0.2535	
2.50	1.0518	1.1067	0.1299	0.3444	
3.00	1.0739	1.1546	0.1530	0.4243	
4.00	1.1159	1.2499	0.1867	0.5632	
5.00	1.1542	1.3416	0.2104	0.6839	
6.00	1.1889	1.4288	0.2381	0.7925	
8.00	1.2497	1.5909	0.2529	0.9045	
10.00	1.3018	1.7392	0.2656	1.1533	
$n = 4$					
1.50	1.0058	1.0181	0.0313	0.1012	0.1432
2.00	1.0162	1.0530	0.0522	0.1744	0.2533
2.50	1.0292	1.0930	0.0672	0.2132	0.3476
3.00	1.0413	1.1342	0.0785	0.2824	0.4327
4.00	1.0642	1.2152	0.0942	0.3630	0.5053
5.00	1.0845	1.2920	0.1046	0.4283	0.7228
6.00	1.1027	1.3641	0.1119	0.4836	0.8500
8.00	1.1339	1.4960	0.1214	0.5746	1.0826
10.00	1.1600	1.6143	0.1271	0.6486	1.2944

TABLE I-6  
IMMITANCES OF BRANCH-GUIDE COUPLINGS FOR  $n = 2, 3$  AND 4 SECTIONS  
(THREE, FOUR, AND FIVE BRANCHES) WHEN  $\psi = 0.80$

$A$	$R_1$	$R_2$	$R_3$	$R_4$	$R_5$
$n = 2$					
1.50	1.0173		0.1225	0.1630	
2.00	1.0508		0.2097	0.2875	
2.50	1.0691		0.2776	0.3933	
3.00	1.1286		0.3333	0.4879	
4.00	1.2062		0.4221	0.6557	
5.00	1.2798		0.4919	0.8049	
6.00	1.3491		0.5497	0.9513	
8.00	1.4760		0.6437	1.1872	
10.00	1.5905		0.7192	1.4075	
$n = 3$					
1.50	1.0114	1.0204	0.0679	0.1361	
2.00	1.0334	1.0525	0.1147	0.2388	
2.50	1.0580	1.1067	0.1495	0.3247	
3.00	1.0830	1.1544	0.1768	0.4004	
4.00	1.1309	1.2499	0.2175	0.5324	
5.00	1.1749	1.3416	0.2468	0.6476	
6.00	1.2153	1.4288	0.2692	0.7513	
8.00	1.2870	1.5909	0.3020	0.9353	
10.00	1.3491	1.7392	0.3254	1.0973	
$n = 4$					
1.50	1.0069	1.0184	0.0374	0.0997	0.1339
2.00	1.0199	1.0540	0.0626	0.1724	0.2368
2.50	1.0344	1.0947	0.0808	0.2309	0.3251
3.00	1.0489	1.1368	0.0947	0.2803	0.4045
4.00	1.0763	1.2196	0.1143	0.3620	0.5472
5.00	1.1009	1.2983	0.1276	0.4288	0.6757
6.00	1.1230	1.3725	0.1372	0.4860	0.7946
8.00	1.1614	1.5083	0.1501	0.5813	1.0119
10.00	1.1939	1.6306	0.1582	0.6598	1.2097

TABLE I-7  
TRANSMISSIONS OF BRANCH-GUIDE COUPLES FOR  $n = 2, 3$  AND 4 SECTIONS  
(THREE, FOUR, AND FIVE BRANCHES) WHEN  $\nu_3 = 1.00$

$n$	$K_1$	$K_2$	$K_3$	$K_4$	$K_5$
$n = 2$					
1.50	1.0183		0.1354	0.1373	
2.00	1.0537		0.2326	0.2418	
2.50	1.0944		0.3091	0.3303	
3.00	1.1364		0.3728	0.4090	
4.00	1.2195		0.4759	0.5440	
5.00	1.2990		0.5549	0.6708	
6.00	1.3742		0.6294	0.7824	
8.00	1.5133		0.7463	0.9821	
10.00	1.6397		0.8432	1.1595	
$n = 3$					
1.50	1.0131	1.0206	0.0607	0.1233	
2.00	1.0393	1.0606	0.1369	0.2165	
2.50	1.0648	1.1067	0.1795	0.2948	
3.00	1.0958	1.1546	0.2134	0.3639	
4.00	1.1521	1.2499	0.2652	0.4847	
5.00	1.2047	1.3116	0.3019	0.5904	
6.00	1.2534	1.4288	0.3347	0.6859	
8.00	1.3412	1.5909	0.3817	0.8556	
10.00	1.4189	1.7392	0.4173	1.0057	
$n = 4$					
1.50	1.0084	1.0188	0.0472	0.0961	0.1214
2.00	1.0246	1.0552	0.0794	0.1661	0.2147
2.50	1.0426	1.0969	0.1030	0.2240	0.2946
3.00	1.0607	1.1400	0.1211	0.2728	0.3665
4.00	1.0952	1.2251	0.1476	0.3545	0.4956
5.00	1.1267	1.3062	0.1661	0.4223	0.6118
6.00	1.1554	1.3828	0.1799	0.5803	0.7191
8.00	1.2057	1.5237	0.1994	0.5802	0.9152
10.00	1.2470	1.6510	0.2127	0.6635	1.0935

TABLE I-8  
IMMITTANCES OF BRANCH-GUIDE COUPLERS FOR  $n = 2, 3$  AND 4 SECTIONS  
(THREE, FOUR, AND FIVE BRANCHES) WHEN  $\mu = 1.20$

$R$	$K_1$	$K_2$	$H_1$	$H_2$	$H_3$
$n = 2$					
1.50	1.0192		0.1533	0.1056	
2.00	1.0565		0.2607	0.1055	
2.50	1.0995		0.3479	0.2327	
3.00	1.1441		0.4212	0.3121	
4.00	1.2325		0.5419	0.4160	
5.00	1.3174		0.6410	0.5067	
6.00	1.3982		0.7263	0.5884	
8.00	1.5481		0.8708	0.7331	
10.00	1.6852		0.9929	0.8601	
$n = 3$					
1.50	1.0152	1.0206	0.0994	0.1046	
2.00	1.0445	1.0606	0.1696	0.1838	
2.50	1.0780	1.1067	0.2238	0.2504	
3.00	1.1123	1.1546	0.2680	0.3092	
4.00	1.1800	1.2202	0.3376	0.4123	
5.00	1.2139	1.3416	0.3918	0.5023	
6.00	1.3040	1.4208	0.4364	0.5841	
8.00	1.4140	1.5909	0.5042	0.7291	
10.00	1.5133	1.7392	0.5657	0.8572	
$n = 4$					
1.50	1.0108	1.0192	0.0631	0.0886	0.1047
2.00	1.0315	1.0566	0.1066	0.1542	0.1851
2.50	1.0518	1.0994	0.1393	0.2080	0.2539
3.00	1.0785	1.1438	0.1650	0.2544	0.3157
4.00	1.1243	1.2316	0.2037	0.3331	0.4263
5.00	1.1667	1.3156	0.2320	0.3995	0.5256
6.00	1.2059	1.3951	0.2541	0.4578	0.6171
8.00	1.2761	1.5419	0.2873	0.5581	0.7937
10.00	1.3301	1.6753	0.3119	0.6437	0.9345

## APPENDIX II

### COUPLING FORMULAS FOR CASCADED MATCHED DIRECTIONAL COUPLERS

When two or more directional couplers are cascaded, as shown in Fig. II-1, the combination is still a directional coupler. When the couplers are matched, the couplings  $P_{1,\text{even}}$  and  $P_{2,\text{even}}$  of the combination can readily be worked out. Let  $P_{1,i}$  and  $P_{2,i}$  be the couplings of the  $i$ th coupler. All the quantities  $P_{1,\text{even}}$ ,  $P_{2,\text{even}}$ ,  $P_{1,i}$ ,  $P_{2,i}$  are supposed to be measured in decibels and are taken as positive numbers. The couplings are determined by the difference in phase shift between the even and the odd modes (Fig. II-2), which is  $2\theta_i$  for the  $i$ th coupler, and is given by

$$\left. \begin{aligned} \text{antilog}\left(\frac{P_{1,i}}{20}\right) &= \sin \theta_i \\ \text{antilog}\left(\frac{P_{2,i}}{20}\right) &= \cos \theta_i \end{aligned} \right\} \quad (II-1)$$

The couplings  $P_{1,\text{even}}$  and  $P_{2,\text{even}}$  of  $N$  such cascaded couplers are then given by

$$\left. \begin{aligned} \text{antilog}\left(\frac{P_{1,\text{even}}}{20}\right) &= \sin \left[ \sum_{i=1}^N \theta_i \right] \\ \text{antilog}\left(\frac{P_{2,\text{even}}}{20}\right) &= \cos \left[ \sum_{i=1}^N \theta_i \right] \end{aligned} \right\} \quad (II-2)$$

For instance two 3-db couplers, or three 6-db couplers, yield one 0-db coupler. To obtain 3-db coupling with two equal couplers, each must have a coupling  $P_2$  of about 8.36 db.

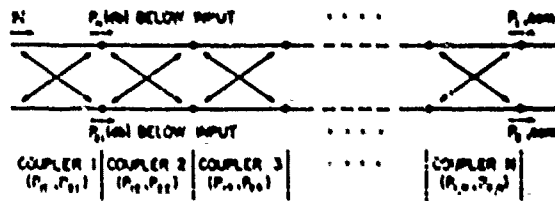
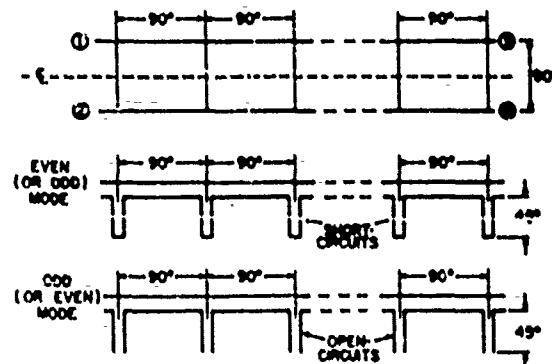


FIG. II-1 SEVERAL MATCHED DIRECTIONAL COUPLERS IN CASCADE



PORT	1	2	3	4
EVEN MODE	↑	↑	$\lambda/4$	$\lambda/4$
ODD MODE	↑	↑	$\pi/4$	$\pi/4$
SUM:	↑	ZERO	↓	→
AMPLITUDE:	1	0	$\cos \theta$	$\sin \theta$
POWER:	1	0	$\cos^2 \theta$	$\sin^2 \theta$

FIG. II-2 SUMMARY OF EVEN- AND ODD-MODE ANALYSIS

## APPENDIX III

### CALCULATION OF CHOKES IN BRANCHES

Consider a length of transmission line of characteristic impedance  $Z_0$ , with a series T-junction in the mid-plane (Fig. III-1). The stub line of characteristic impedance  $Z_1$  is shorted at the other end. (The line  $Z_1$  will be the branch guide, and the stub  $Z_2$  will be the choke.) The electrical length  $\theta_2$  of the stub will be chosen to be 90 degrees long at 2600 Mc (the second harmonic of the center frequency). Its impedance  $Z_2$

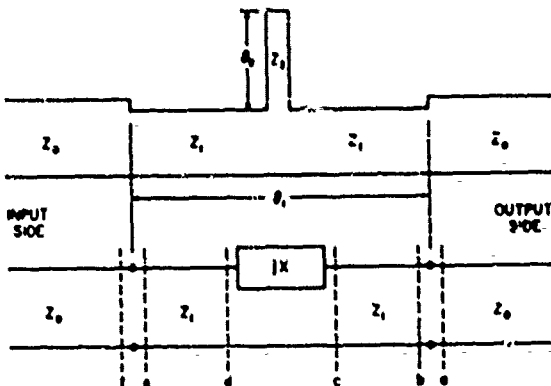


FIG. III-1 TRANSMISSION-LINE STUB IN THE MID-PLANE  
OF A LINE ONE-QUARTER WAVELENGTH LONG

is determined from the bandwidth over which the reflection shall exceed some minimum specified value. In this case it was decided that a minimum attenuation of 4 db over a 20 percent fractional bandwidth (in reciprocal guide wavelength) would be sufficient. The stub electrical length  $\theta_2$  then changes by 19 degrees from 90 degrees, and  $Z_2/Z_1$  turns out to be equal to 0.4 to give 4 db attenuation at the 20 percent band edges. Such a stub presents a series reactance  $X$  at 1300 Mc whose normalized value is equal to

$$X = \frac{Z_2}{Z_1} \tan \left[ \left( \frac{\lambda_s \text{ at } 2600 \text{ Mc}}{\lambda_s \text{ at } 1300 \text{ Mc}} \right) 90^\circ \right] . \quad (III-1)$$

The problem now is to find the value of  $Z_1/Z_0$ , such that for the given electrical length  $\theta_1$  of the line  $Z_1$  (Fig. III-1), the input is matched, when the output is matched, at 1300 Mc. It is possible to solve this problem for any value of  $\theta_1$ . In this case  $\theta_1$  was nominally equal to 90 degrees at 1300 Mc, but it was not clear how much to allow for the T-junction reference planes, which in any case would move as  $Z_1$  is changed. For this reason  $\theta_1$  was simply taken as 90 degrees at 1300 Mc.

The matching procedure at center frequency (1300 Mc) can be seen on a Smith chart (Fig. III-2). The letters correspond to the similarly marked cross-sections in Fig. III-1. The points *c* and *d* are on the horizontal diameter (broken line) because  $\theta_1$  has been taken as 90 degrees at center frequency. One moves from point *c* to point *d* by adding a reactance  $X$  given by Eq. (III-1). The end-point *f*, like the starting-point *e*, is in the center of the Smith chart, signifying a match ( $VSWR = 1.0$ ). It remains to relate  $Z_1/Z_0$ , the impedance at *b* or *e* in Fig. III-2 to  $X$ .

The impedances at *c* and *d* in Fig. III-2 are complex conjugates and are given by

$$Z_c \text{ or } d = R_c \pm jX_c \quad (III-2)$$

where

$$R_c = \sqrt{1 - X_c^2} . \quad (III-3)$$

since on the horizontal diameter (broken line)

$$R_c^2 + X_c^2 = 1 . \quad (III-4)$$

The addition of a reactance  $X$  causes  $Z_c$  to become  $Z_d$  (symmetrically placed in Fig. III-2), and therefore

$$X_c = -X_d = -X/2 . \quad (III-5)$$

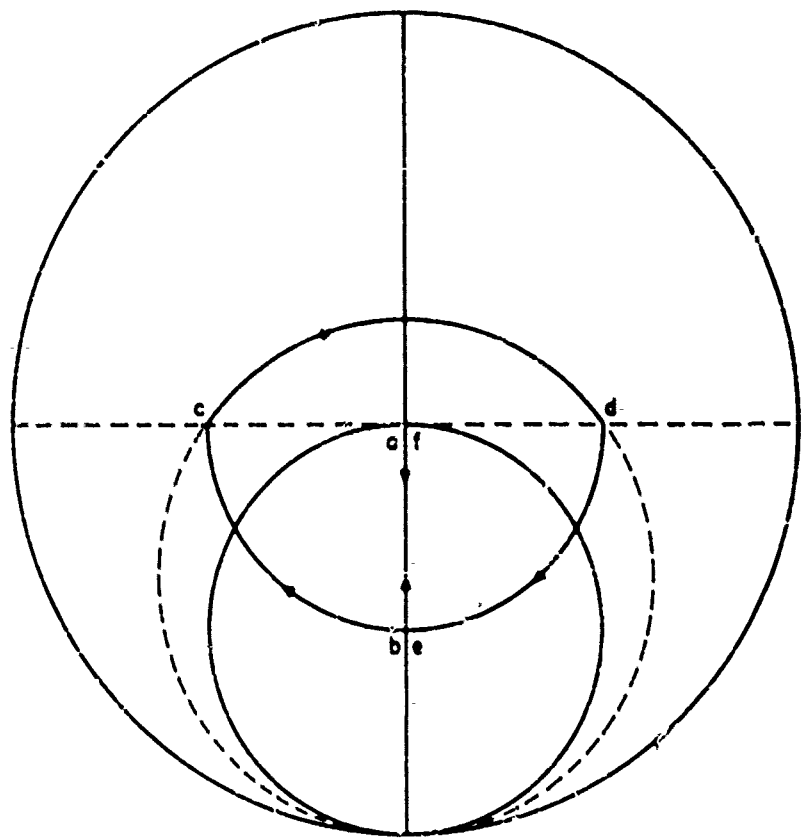


FIG. III-2 SMITH CHART PROCEDURE TO FIND  $Z_1$  OF FIG. C-1  
TO MATCH THE STUB  $Z_2$

Moreover, the reflection coefficient amplitude at c or d in Fig. III-2 can be shown to be given by

$$|\Gamma_c|^2 = \frac{1 - R_c}{1 + R_c} \quad (III-6)$$

and  $|\Gamma_c|$  is the same reflection coefficient as at b, where the normalized impedance  $Z_0/Z_1$  is also equal to the VSWR. Therefore

$$\frac{Z_0}{Z_1} = \frac{1 + |\Gamma_c|}{1 - |\Gamma_c|} \quad (III-7)$$

Combining Eqs. (III-1) through (III-7),

$$\frac{Z_1}{Z_0} = \frac{(1+A)^X - (1-A)^X}{(1+A)^X + (1-A)^X} \quad (III-8)$$

where

$$A^2 = 1 - (X/2)^2$$

and  $X$  is given by Eq. (III-1), with  $Z_1/Z_0$  equal to 0.4 in this case. The branch waveguide heights in Fig. 30 have accordingly to be reduced in the ratio of the appropriate  $Z_1/Z_0$  given by Eq. (III-8). With a guide wavelength of 4.84 inches at 2600 Mc, and of 12.68 inches at 1300 Mc, Eq. (III-1) yields  $X = 0.274$ . Then from Eq. (III-8),  $(Z_1/Z_0) = 0.872$ .

To minimize junction effects, symmetrical chokes were used in all but the narrowest branches (see photograph Fig. 34). The final dimensions are shown in Fig. 33. The stub lengths in some branches are not the same on both sides, where they are 1.200 inches on one side and 1.090 inches on the other: this was done for mechanical reasons, to leave more material around the center of the smaller block 'C' (Fig. 33), which held the bolt fastening the block down. This slight unbalance in choke lengths should have the effect of stagger-tuning, and should not affect electrical performance appreciably.

The insertion loss characteristic of the complete coupler with the chokes has already been given in Fig. 35.

STANFORD  
RESEARCH  
INSTITUTE

MENLO PARK  
CALIFORNIA

## Regional Offices and Laboratories

**Southern California Laboratories**  
820 Mission Street  
South Pasadena, California

**Washington Office**  
308 17th Street, N.W.  
Washington 5, D.C.

**New York Office**  
270 Park Avenue, Room 1770  
New York 17, New York

**Detroit Office**  
The Stevens Building  
1025 East Maple Road  
Birmingham, Michigan

**European Office**  
Mühikanstrasse 37  
Zurich 1, Switzerland

**Japan Office**  
911 Iino Building  
22, 2-chome, Uchisaiwai-cho, Chiyoda-ku  
Tokyo, Japan

## Representatives:

**Honolulu, Hawaii**  
Finance Factors Building  
155 South King Street  
Honolulu, Hawaii

**London, England**  
19 Upper Brook Street  
London, W. 1, England

**Milan, Italy**  
Via Macedonio Melloni 40  
Milan, Italy